

Applicants: Paz Einat, et al.
Serial No.: 10/618,143
Filed: July 11, 2003
Page 4

Amendments to the Drawings:

Please replace Figures 1-10 with the replacement versions of Figures 1-10 (12 replacement sheets) attached hereto as **Exhibit B.**

Applicants: Paz Einat, et al.
Serial No.: 10/618,143
Filed: July 11, 2003
Page 13

REMARKS

By this Amendment, applicants have amended the specification to add a sequence identifier on page 39, line 151 to correct an obvious typographical error in the sequence listed on page 39, line 15; and to correct the descriptions of Figures 7-9 in the Brief Description of the Figures on page 31. Support for the amendment to the brief descriptions of Figures 7 and 8 may be found on page 38, line 25 to page 39, line 10. The amendment to the description of Figure 9 is a minor stylistic change. Applicants maintain that these amendments to the specification raise no issue of new matter and respectfully request that the Examiner enter these amendments.

By this Amendment, applicants have also amended the drawings and attach hereto as **Exhibit B** twelve (12) replacement sheets containing replacement versions of Figures 1-12. Specifically, applicants have renumbered the figures on sheets 1/12 and 2/12 as Figure 1A and Figure 1B, respectively. Applicants have also renumbered the figures on sheets 6/12 and 7/12 as Figure 5A and Figure 5B, respectively. Applicants have relabeled the figures on sheet 11/12 as Figure 9A and Figure 9B. Applicants have also amended Figure 8 (sheet 10/12) to provide a description of IRT_4C1 in accordance with the December 14, 2006 Office Action. Support for the amendment to Figure 8 is found on page 38, line 25 to page 39, line 10, and in Figure 5. Applicants maintain that these amendments to the drawings raise no issue of new matter and respectfully request that the Examiner enter the replacement sheets of figures.

Claims 1-26 are pending in the subject application. Claims 1, 2, 6, 7, 11, 25 and 26 are under examination. Claims 3-5, 8-10, and 12-24 are withdrawn. By this Amendment, applicants have added new claims 27 and 28, and amended claims 1-19, 25 and 26. Support for new

Applicants: Paz Einat, et al.

Serial No.: 10/618,143

Filed: July 11, 2003

Page 14

claims 27-28 may be found in the specification, *inter alia*, on page 14, lines 26-28; page 15, lines 29-30; page 16, lines 18-20; and page 17, lines 1-3. Support for amended claims 1, 7, 25, and 26 may be found on page 17, lines 25-29. No issue of new matter is raised by these amendments. Accordingly, applicants respectfully request entry of this Amendment. Upon entry of this Amendment, claims 1-28 will be pending in the subject application. Of these, claims 1, 2, 6, 7, 11, and 25-28 will be under examination.

Objections to the Specification

The Examiner objected to the Amendment filed November 3, 2006, under 35 U.S.C. §132(a) as allegedly introducing new matter. In response, applicants note that the November 3, 2006 Amendment was submitted to correct a typographical error in a sequence in Figure 4 which was labeled as an siRNA sequence but written as a DNA sequence. The original Figure 4, which depicted the sequence of an siRNA according to SEQ ID NO:6, inadvertently included thymidine, a deoxyribonucleotide, rather than uracil, the corresponding ribonucleotide.

Applicants respectfully disagree with the Examiner and maintain that this error was an obvious typographical error. Support for the amendment can be found throughout the specification. siRNA molecules are known in the art as molecules composed of ribonucleotides, and not deoxyribonucleotides. The present specification states that siRNA refers to "an RNA molecule which decreases or silences the expression of a gene/ mRNA of its endogenous or cellular counterpart" (page 4, lines 17-19). Furthermore, the specification states: "[W]hen RNA sequences are said to be similar, or to have a degree of sequence identity or homology with DNA sequences, thymidine (T) in the DNA sequence is

Applicants: Paz Einat, et al.

Serial No.: 10/618,143

Filed: July 11, 2003

Page 15

considered equal to uracil (U) in the RNA sequence. RNA sequences within the scope of the invention can be derived from DNA sequences or their complements, by substituting thymidine (T) in the DNA sequence with uracil (U). RNA sequences within the scope of the invention can be derived from DNA sequences or their complements, by substituting thymidine (T) in the DNA sequence with uracil (U)" (page 29, lines 19-25).

Thus, it is clear from the present application that the sequence identified as SEQ ID NO:6 is an siRNA, and that an amendment changing the *T* nucleotides to *U* nucleotides is not new matter because (i) it is clear from the subject application that the sequence identified as SEQ ID NO:6 is the sequence of an RNA, not DNA; (ii) RNA sequences do not contain *T*, but *U* instead; and (iii) the error was typographical in nature.

Applicants have herein amended the specification to change the *T* nucleotides to *U* nucleotides in the sequence listed on page 39, line 15. Applicants note that this sequence is an siRNA sequence identified as SEQ ID NO: 6. Applicants maintain that this sequence erroneously contained *T* nucleotides instead of *U* nucleotides due to a typographical error. For the reasons stated in the paragraphs above, it is clear from the present application that applicants intended the sequence listed on page 39, line 15, to be an siRNA, and that an amendment changing the *T* nucleotides to *U* nucleotides does not constitute new matter. Accordingly, applicants respectfully request that the Examiner enter this amendment.

The Examiner objected to the specification as allegedly failing to comply with the requirements of 37 C.F.R. §1.821-1.825. Specifically, the Examiner indicated that a sequence identifier is required for the sequence on page 39, line 15, as also indicated in

Applicants: Paz Einat, et al.
Serial No.: 10/618,143
Filed: July 11, 2003
Page 16

the accompanying Notice to Comply with Requirements for Patent Applications Containing Nucleotide and/or Amino Acid Sequence Disclosures. A copy of the Notice to Comply is attached hereto as **Exhibit A**.

In response, applicants have amended the specification to add the appropriate sequence identifier. Applicants maintain that no new matter has been added and therefore a substitute Sequence Listing is not required.

The Examiner further objected to the specification because the word "polynucleotides" is misspelled in the heading on page 54. Applicants note that the word "polynucleotides" is correctly spelled in the heading on page 54 of the application as filed. Applicants note that the typographical error appears in the published document, i.e. U.S. Patent Application Publication No. 2004/0067234 A1. Specifically, in the heading preceding paragraph [0267] of the published document, the word "polynucleotides" is misspelled as "Polynucle Tides." Applicants maintain that the subject application as filed does not include this typographical error, and therefore no amendment is required.

Objections to the Drawings

The Examiner objected to Figure 8 under 37 C.F.R. §1.121(d) as lacking a definition of IRT_4C1. In response, applicants attach hereto as **Exhibit B** twelve (12) replacement drawings in which applicants have amended Figure 8 to describe IRT_4C1 as the IDH antisense fragment. Applicants have also amended the Brief Description of Figure 8. Support for these amendments may be found on page 38, line 25 to page 39, line 10, and in Figure 5. Applicants draw the Examiner's attention to Figure 5 and the legend

Applicants: Paz Einat, et al.
Serial No.: 10/618,143
Filed: July 11, 2003
Page 17

thereto. Figure 5 shows the alignment of the isocitrate dehydrogenase (IDH) gene and the sense sequence of the IDH antisense fragment. The antisense fragment is labeled as IRT-4C1 in Figure 5. Applicants maintain that it is therefore clear that IRT-4C1 is the antisense fragment of IDH. Applicants also draw the Examiner's attention to the specification on page 38, line 25 to page 39, line 10, which refers to loss of function experiments conducted with the IDH antisense fragment, i.e. IRT_4C1. Applicants maintain that these amendments raise no issue of new matter.

In view of these amendments and the remarks above, applicants maintain that the replacement drawings comply with the requirements of 37 C.F.R. §1.121(d) and respectfully request that the Examiner reconsider and withdraw this ground of rejection.

Claim Rejections under 35 U.S.C. §112, first paragraph

Enablement

The Examiner rejected claims 1, 2, 6, 7, 11, 25 and 26 under 35 U.S.C. §112, first paragraph, as containing subject matter which was not described in the specification in such a way as to enable one skilled in the art to make and/or use the invention.

Specifically, the Examiner alleged that (1) no nexus has been established between the inhibition of the IDH polypeptide and any apoptosis related disease because the artifactual nature of the cultured cells is well known in the art and the unpredictability of drug development for apoptosis related disease is also well known in the art; and (2) no nexus has been established between the treatment of the cells with siRNA for the IDH gene and an effect on the IDH polypeptide.

Applicants: Paz Einat, et al.

Serial No.: 10/618,143

Filed: July 11, 2003

Page 18

In response, applicants respectfully traverse the Examiner's rejection.

With regard to the Examiner's first point, applicants maintain that the disclosure of the subject specification and the knowledge in the art provide sufficient guidance for one skilled in the art to readily use the claimed invention. Specifically, applicants draw the Examiner's attention to the specification on page 21, line 16 to page 22, line 17, which discloses an *in vivo* application of the subject invention. In addition, by way of example, the specification discloses that *ex vivo* gene therapy requires the isolation and purification of patient cells, the introduction of a therapeutic gene, and the introduction of genetically altered cells into the patient. The specification also discloses several approaches to *in vivo* gene therapy such as "packaging" the therapeutic gene for administration to a patient in liposomes or in a replication-deficient virus, directly injecting the therapeutic gene into the bloodstream, or introducing the therapeutic gene into the target tissue by microparticle bombardment. The specification further discloses that gene therapy vectors can be delivered to a patient by, for example, intravenous injection, local administration, or stereotactic injection.

Applicants further note that experimental data demonstrating the inhibition of IDH expression promoting cell death is provided *inter alia* in the subject specification. Several experimental systems were used to show the direct link between inhibition of IDH and apoptosis. Example IIC on pages 39-40 of the subject application discloses a gain of function assay which demonstrates that IDH expression protects cells from apoptosis. The results are depicted as the percentage of cells protected from apoptosis (Figure 9A) and the percentage of cell survival (Figure 9B), following anti-Fas

Applicants: Paz Einat, et al.

Serial No.: 10/618,143

Filed: July 11, 2003

Page 19

induced apoptosis in cells ectopically expressing IDH. The inhibition assays further corroborate this result. In addition, the subject application discloses at page 14 examples of small molecules that are inhibitors of IDH. Example IV on pages 44-50 of the subject application discloses screening assays for identifying and isolating IDH inhibitors.

In addition, applicants have submitted herewith documents which further substantiate the nexus between expression of IDH and tumorigenesis in various tissue types. Document number 1 (attached hereto as **Exhibit 1**) establishes that the expression of fifteen proteins including IDH1 was up-regulated in esophageal squamous cell carcinoma tissue compared to the expression in adjacent normal epithelium. Document number 2 (attached hereto as **Exhibit 2**) discloses that microarray analysis identified a 41-fold up-regulation of the expression of IDH1 in non-functional pituitary adenomas.

Accordingly, applicants maintain that a definite nexus exists between the inhibition of the IDH polypeptide and apoptosis-related diseases as shown in the documents submitted herewith.

With regard to the Examiner's second point, applicants maintain that the specification discloses the nexus between the treatment of cells and the effect on the IDH polypeptides now claimed. Specifically, as disclosed in Example IIA on pages 38-39 and in Figures 7 and 8 of the subject application, antisense treatment created greater sensitivity to FAS-mediated apoptosis and Doxorubicin-mediated apoptosis in HeLa cells which were stably transfected with a vector harboring an IDH1 specific antisense molecule (IRT-4C1) than in "control" HeLa cells transfected with an empty vector. The subject application also discloses in Example IIB

Applicants: Paz Einat, et al.

Serial No.: 10/618,143

Filed: July 11, 2003

Page 20

on page 39 that transiently transfecting HeLa cells with an IDH siRNA induced apoptosis in the HeLa cells when they were treated with doxorubicin.

Applicants again draw the Examiner's attention to the results presented in Example II (pages 38-40), in which ectopic expression of IDH results in protection of cells from apoptosis. Furthermore, inhibition of IDH with either an antisense or an siRNA molecule leads to increased sensitivity of cells to apoptosis. Applicants maintain that the siRNA results are corroborated with antisense results, demonstrating siRNA specificity for the IDH gene.

On page 11 of the Office Action, the Examiner stated that while being enabling for a method of treatment of an apoptosis-related disease or for potentiating a chemotherapeutic treatment of an apoptosis-related disease in a subject comprising administering to the subject a therapeutically effective amount of an inhibitor of the IDH polypeptide, wherein the IDH polypeptide is SEQ ID NO: 2 or 4, in a dosage sufficient to inhibit IDH so as to thereby treat the subject, wherein the IDH inhibitor is an siRNA for the IDH gene, wherein the IDH gene is SEQ ID NO:1 or 3, the specification does not reasonably provide enablement for a method of treatment of an apoptosis-related disease or for potentiating a chemotherapeutic treatment of an apoptosis-related disease in a subject comprising administering to the subject a therapeutically effective amount of an inhibitor of the IDH polypeptide, in a dosage sufficient to inhibit IDH so as to thereby treat the subject, wherein the IDH inhibitor is an siRNA for the IDH gene. The Examiner also stated that the single siRNA taught in the specification would not be expected to inhibit the scope of IDH polypeptides contemplated.

In response, applicants note that amended claims 1, 7, 25 and 26 recite the IDH polypeptide as an IDH polypeptide having a sequence

Applicants: Paz Einat, et al.

Serial No.: 10/618,143

Filed: July 11, 2003

Page 21

as set forth in SEQ ID NO:2 or SEQ ID NO:4 or having a sequence modified therefrom while retaining the biological properties of IDH. Applicants maintain that the claimed modified IDH polypeptides do not include any and every homolog of the IDH polypeptide. Rather, the claimed modified IDH polypeptides must be related to the IDH polypeptides identified by SEQ ID NO:2 or SEQ ID NO:4 while retaining the biological properties of IDH. Applicants note that the Examiner's assertion that alterations of even a single amino acid in a polypeptide sequence can, in some cases, dramatically affect the biological activity and characteristics of the protein is therefore moot, because the claimed modified IDH polypeptides retain the biological activity of the IDH polypeptide.

Accordingly, for the reasons stated above, applicants maintain that the specification of the subject application satisfies the requirements of 35 U.S.C. §112, first paragraph.

Written Description

The Examiner rejected claims 1, 2, 6, 7, 11, 25 and 26 under 35 U.S.C. §112, first paragraph, as lacking an adequate written description. Specifically, the Examiner alleged that the specification does not describe (i) the broadly claimed IDH polypeptides to be inhibited; and (ii) the broadly claimed siRNA for the IDH gene.

In response, applicants respectfully traverse the Examiner's ground of rejection. As stated above, applicants have herein amended claims 1, 7, 25 and 26 to recite the IDH polypeptide having a sequence as set forth in SEQ ID NO:2 or SEQ ID NO:4 or having a sequence modified therefrom while retaining the biological properties of IDH. Applicants maintain that the specification adequately describes the claimed genus of IDH polypeptides (see

Applicants: Paz Einat, et al.

Serial No.: 10/618,143

Filed: July 11, 2003

Page 22

inter alia, page 6, line 14 to page 7, line 5; page 11, lines 23-33; and Figures 1, 2, and 6). Applicants again maintain that the claimed modified IDH polypeptides do not include *any and every* homolog of the IDH polypeptide. Rather, the claimed modified IDH polypeptides are related to the IDH polypeptides identified by SEQ ID NO:2 or SEQ ID NO:4 while retaining the biological properties of IDH.

In addition, applicants have herein amended claims 25 and 26 and added new claims 27 and 28 to recite the siRNA comprising nucleotides have a sequence as set forth in SEQ ID NO:6. Applicants maintain that the specification adequately describes the claimed genus of siRNA (see *inter alia*, page 4, lines 17-28; page 14, lines 26-28; page 15, line 19 to page 17, line 7; page 39, lines 12-21; and Figure 4). Applicants maintain that the claimed siRNAs do not include siRNAs specific to *any and every* homolog of the IDH polypeptide, but only those siRNAs specific to the IDH polypeptides of SEQ ID NO: 2 or SEQ ID NO: 4 or having a sequence modified therefrom while retaining the biological activity of the IDH polypeptide.

Accordingly, for the reasons stated above, applicants maintain that the specification of the subject application satisfies the requirements of 35 U.S.C. §112, first paragraph.

Applicants: Paz Einat, et al.
Serial No.: 10/618,143
Filed: July 11, 2003
Page 23

SUPPLEMENTAL INFORMATION DISCLOSURE STATEMENT

In accordance applicants' duty of disclosure under 37 C.F.R. §1.56 and §1.97(a)-(d), applicants submit this Supplemental Information Disclosure Statement to supplement the Information Disclosure Statement filed March 2, 2004. Applicants direct the Examiner's attention to the following references which are listed on the Substitute Form PTO-1449 attached hereto as **Exhibit B**:

1. Qi, Y., et al., (2005) Comparative proteomic analysis of esophageal squamous cell carcinoma. *Proteomics* 5(11):2960-71 (**Exhibit 1**); and
2. Moreno, C.S., et al., (2005) Novel molecular signaling and classification of human clinically nonfunctional pituitary adenomas identified by gene expression profiling and proteomic analyses. *Cancer Res.* 65(22):10214-22 (**Exhibit 2**).

Copies of documents numbers 1 and 2 are attached hereto as **Exhibits 1 and 2**, respectively.

The Examiner is respectfully requested to make the above-listed references of record in the present application by initialing and dating the attached Substitute Form PTO-1449, and returning a copy of the initialed and dated form to applicants' undersigned attorney.

This Supplemental Information Disclosure Statement is being submitted pursuant to 37 C.F.R. §1.97(c)(2) before the mailing of a Final Office Action. Pursuant to 37 C.F.R. §1.17(p), the fee for filing this Supplemental Information Disclosure Statement is ONE HUNDRED AND EIGHTY DOLLARS (\$180.00) and a check including this

Applicants: Paz Einat, et al.
Serial No.: 10/618,143
Filed: July 11, 2003
Page 24

amount is enclosed.

If a telephone interview would be of assistance in advancing prosecution of the subject application, applicants' undersigned attorney invites the Examiner to telephone him at the number provided below.

No fee, other than the enclosed fee of \$740.00, including \$510.00 for a three-month extension of time; \$180.00 for filing the Supplemental Information Disclosure Statement; and \$50.00 for two (2) additional claims, is deemed necessary in connection with the filing of this Amendment. If any additional fee is required, authorization is hereby given to charge the amount of any such fee to Deposit Account No. 03-3125.

Respectfully submitted,



John P. White
Registration No. 28,678
Attorney for Applicants
Cooper & Dunham LLP
1185 Avenue of the Americas
New York, New York 10036
(212) 278-0400

I hereby certify that this correspondence is being deposited this date with the U.S. Postal Service with sufficient postage as first class mail in an envelope addressed to: Mail Stop Amendment, Commissioner For Patents, P.O. Box 1450, Alexandria, VA 22313-1450


John P. White
Reg. No. 28,678

6/14/07
Date

EXHIBIT A

**Applicants: Paz Einat, et al.
U.S. Serial No.: 10/618,143
Filed: July 11, 2003**

Notice to Comply	Application No. 10/618,143	Applicant(s) Einat et al.	
	Examiner Peter J. Reddig	Art Unit 1642	
NOTICE TO COMPLY WITH REQUIREMENTS FOR PATENT APPLICATIONS CONTAINING NUCLEOTIDE SEQUENCE AND/OR AMINO ACID SEQUENCE DISCLOSURES			
<p>Applicant must file the items indicated below within the time period set the Office action to which the Notice is attached to avoid abandonment under 35 U.S.C. § 133 (extensions of time may be obtained under the provisions of 37 CFR 1.136(a)).</p> <p>The nucleotide and/or amino acid sequence disclosure contained in this application does not comply with the requirements for such a disclosure as set forth in 37 C.F.R. 1.821 - 1.825 for the following reason(s):</p> <ul style="list-style-type: none"> <input checked="" type="checkbox"/> 1. This application clearly fails to comply with the requirements of 37 C.F.R. 1.821-1.825. Applicant's attention is directed to the final rulemaking notice published at 55 FR 18230 (May 1, 1990), and 1114 OG 29 (May 15, 1990). If the effective filing date is on or after July 1, 1998, see the final rulemaking notice published at 63 FR 29620 (June 1, 1998) and 1211 OG 82 (June 23, 1998). <input type="checkbox"/> 2. This application does not contain, as a separate part of the disclosure on paper copy, a "Sequence Listing" as required by 37 C.F.R. 1.821(c). <input type="checkbox"/> 3. A copy of the "Sequence Listing" in computer readable form has not been submitted as required by 37 C.F.R. 1.821(e). <input type="checkbox"/> 4. A copy of the "Sequence Listing" in computer readable form has been submitted. However, the content of the computer readable form does not comply with the requirements of 37 C.F.R. 1.822 and/or 1.823, as indicated on the attached copy of the marked-up "Raw Sequence Listing." <input type="checkbox"/> 5. The computer readable form that has been filed with this application has been found to be damaged and/or unreadable as indicated on the attached CRF Diskette Problem Report. A Substitute computer readable form must be submitted as required by 37 C.F.R. 1.825(d). <input type="checkbox"/> 6. The paper copy of the "Sequence Listing" is not the same as the computer readable form of the "Sequence Listing" as required by 37 C.F.R. 1.821(e). <input checked="" type="checkbox"/> 7. Other: The disclosure is lacking numerous sequence identifiers and sequence ID numbers, see the section titled "Sequence Listing" in the accompanying First Office Action on the Merits. <p>Applicant Must Provide:</p> <ul style="list-style-type: none"> <input type="checkbox"/> An initial or substitute computer readable form (CRF) copy of the "Sequence Listing". <input type="checkbox"/> An initial or substitute paper copy of the "Sequence Listing", as well as an amendment specifically directing its entry into the application. <input type="checkbox"/> A statement that the content of the paper and computer readable copies are the same and, where applicable, include no new matter, as required by 37 C.F.R. 1.821(e) or 1.821(f) or 1.821(g) or 1.825(b) or 1.825(d). <p>For questions regarding compliance to these requirements, please contact:</p> <p>For Rules Interpretation, call (703) 308-4216 or (703) 308-2923 For CRF Submission Help, call (703) 308-4212 or 308-2923 PatentIn Software Program Support Technical Assistance.....703-287-0200 To Purchase PatentIn Software.....703-306-2600</p> <p>PLEASE RETURN A COPY OF THIS NOTICE WITH YOUR REPLY</p>			

Applicants: Paz Einat, et al.
 U.S. Serial No.: 10/618,143
 Filed: July 11, 2003

EXHIBIT B

Applicants: Paz Einat, et al.
U.S. Serial No.: 10/618,143
Filed: July 11, 2003

1/12

Figure 1A

ORF of Isocitrate dehydrogenase 1 (XM_055088)

(nucleic acid sequence: SEQ ID NO:1; amino acid sequence: SEQ ID NO:2)

1	GGC GGC GAA GCG GGG GCA CGC CCT CGC ACA CGC AGA GAT AAA TTG	45
46	TGC TCC CAT GAC CTT TAT TTG GAA AGT GCC TGC GGG CCT AAA ATT	90
91	GGC CTT TGT CCC ACC GAG TAC ACT CAG CAC TGT ACT TTA AAC CGG	135
136	ATA AAC TGG GCT GTC TGG CAG GCG ATA AAC TAC ATT CAG TTG AGT	180
181	CTG CAA GAC TGG GAG GAA CTG GGG TGA TAA GAA ATC TAT TCA CTG	225
226	TCA AGG TTT ATT GAA GTC AAA ATG TCC AAA AAA ATC AGT GGC GGT	270
	M S K K I S G G	8
271	TCT GTG GTA GAG ATG CAA GGA GAT GAA ATG ACA CGA ATC ATT TGG	315
9	S V V E M Q G D E M T R I I W	23
316	GAA TTG ATT AAA GAG AAA CTC ATT TTT CCC TAC GTG GAA TTG GAT	360
24	E L I K E K L I F P Y V E L D	38
361	CTA CAT AGC TAT GAT TTA GGC ATA GAG AAT CGT GAT GCC ACC AAC	405
39	L H S Y D L G I E N R D A T N	53
406	GAC CAA GTC ACC AAG GAT GCT GCA GAA GCT ATA AAG AAG CAT AAT	450
54	D Q V T K D A A E A I K K H N	68
451	GTT GGC GTC AAA TGT GCC ACT ATC ACT CCT GAT GAG AAG AGG GTT	495
69	V G V K C A T I T P D E K R V	83
496	GAG GAG TTC AAG TTG AAA CAA ATG TGG AAA TCA CCA AAT GGC ACC	540
84	E E F K L Q M W K S P N G T	98
541	ATA CGA AAT ATT CTG GGT GGC ACG GTC TTC AGA GAA GCC ATT ATC	585
99	I R N I L G G T V F R E A I I	113
586	TGC AAA AAT ATC CCC CGG CTT GTG AGT GGA TGG GTA AAA CCT ATC	630
114	C K N I P R L V S G W V K P I	128
631	ATC ATA GGT CGT CAT GCT TAT GGG GAT CAA TAC AGA GCA ACT GAT	675
129	I I G R H A Y G D Q Y R A T D	143
676	TTT GTT GTT CCT GGG CCT GGA AAA GTA GAG ATA ACC TAC ACA CCA	720
144	F V V P G P G K V E I T Y T P	158
721	AGT GAC GGA ACC CAA AAG GTG ACA TAC CTG GTA CAT AAC TTT GAA	765
159	S D G T Q K V T Y L V H N F E	173
766	GAA GGT GGT GGT GTT GCC ATG GGG ATG TAT AAT CAA GAT AAG TCA	810
174	E G G G V A M G M Y N Q D K S	188
811	ATT GAA GAT TTT GCA CAC AGT TCC TTC CAA ATG GCT CTG TCT AAG	855
189	I E D F A H S S F Q M A L S K	203
856	GGT TGG CCT TTG TAT CTG AGC ACC AAA AAC ACT ATT CTG AAG AAA	900
204	G W P L Y L S T K N T I L K K	218
901	TAT GAT GGG CGT TTT AAA GAC ATC TTT CAG GAG ATA TAT GAC AAG	945
219	Y D G R F K D I F Q E I Y D K	233
946	CAG TAC AAG TCC CAG TTT GAA GCT CAA AAG ATC TGG TAT GAG CAT	990
234	Q Y K S Q F E A Q K I W Y E H	248
991	AGG CTC ATC GAC GAC ATG GTG GCC CAA GCT ATG AAA TCA GAG GGA	1035
249	R L I D D M V A Q A M K S E G	263
1036	GGC TTC ATC TGG GCC TGT AAA AAC TAT GAT GGT GAC GTG CAG TCG	1080
264	G F I W A C K N Y D G D V Q S	278
1081	GAC TCT GTG GCC CAA GGG TAT GGC TCT CTC GGC ATG ATG ACC AGC	1125
279	D S V A Q G Y G S L G M M T S	293
1126	GTG CTG GTT TGT CCA GAT GGC AAG ACA GTA GAA GCA GAG GCT GCC	1170
294	V L V C P D G K T V E A E A A	308

2 / 12

Figure 1B

3/12

Figure 2:

ORF of Isocitrate dehydrogenase 2 (NM_002168)

(nucleic acid sequence: SEQ ID NO:3; amino acid sequence: SEQ ID NO:4)

1 ccagcgtagcccgccaggcagccgggaggagcggcgctcgacacctctccgc
61 cctgctcgcttcagcttggatgcggctacctcgccgtcgctcgct
1 M A G Y L R V V R S L
121 gcagagcctcaggctcgccggccactatgccgacaaaagatcaagggtggcgaagccctgtgg
12 C R A S G S R P A W A P A A L T A P T S
181 aagagcagccgcggccactatgccgacaaaagatcaagggtggcgaagccctgtgg
32 Q E Q P R R H Y A D K R I K V A K P V V
241 agatggatggatggatggatgaccgtattatctgcagttcatcaaggagaagctcatcc
52 E M D G D E M T R I I W Q F I K E K L I
301 tgccccacgtggacatccagactaaagtatttgaccctcgccaaaccgtgaccaga
72 L P H V D I Q L K Y F D L G L P N R D Q
361 ctgtgaccaggtcacattgactctgcactggccacccagaatgtggctgtca
92 T D D Q V T I D S A L A T Q K Y S V A V
421 agtgtgccaccatccccgtatgaggcccgtgttggaaagatgtcaagctgaagaagatgt
112 K C A T I T P D E A R V E E F K L K K M
481 gaaaaagtcccaatggaaactatccggAACATCCTGGGGGGACTGTCTCCGGGAGCCCA
132 W K S P N G T I R N I L G G T V F R E P
541 tcatctgaaaaacatcccacgcctagtcctggctggaccAAAGCCATCACCATTGGCA
152 I I C K N I P R L V P G W T K P I T I G
601 ggcacgccccatggcgaccagtacaaggccacagactttgtggcagaccggccggcactt
172 R H A H G D Q Y K A T D F V A D R A G T
661 tcaaaatggtcttcacccaaaagatggcagtgggtcaaggaggtggaaagtgtacaact
192 F K M V F T P K D G S G V K E W E V Y N
721 tccccgcaggcggcgtggcatggcatgtacaacaccgacgagtccatctcaggTTG
212 F P A G G V G M G M Y N T D E S I S G F
781 cgcacagctgtccagtatgccatccagaagaaaatggccgtgtacatgagcaccaga
232 A H S C F Q Y A I Q K K W P L Y M S T K
841 acaccatactggaaagcctacgtggcgTTcaaggacatctccaggagatcttgaca
252 N T I L K A Y D G R F K D I F Q E I F D
901 agcaactataagaccgacttcgacaagaataagatctgttatgagcaccggcttattgt
272 K H Y K T D F D K N K I W Y E H R L I D
961 acatggtggctcaggctcaagtctcggtggcttgcggactatg
292 D M V A Q V L K S S G F V W A C K N Y
1021 acggagatgtgcagtccacatctggcccagggtggcttgcggactatg
312 D G D V Q S D I L A Q G F G S L G L M T
1081 ccgtcctggctgcctgatggaaagacgattggggctgatggaccgtca
332 S V L V C P D G K T I E A E A A H G T V
1141 cccgccactatgggagcaccagaagggccggccaccagcaccaacccatcgccagca
352 T R H Y R E H Q K G R P T S T N P I A S
1201 tcttgcctggacacgtggcctggagcacccgggaaagctggatggaaaccaagaccta
372 I F A W T R G L E H R G K L D G N Q D L
1261 tcaggttgcctggagatgtggagaagggtgtgcggagacggggatggagccatga
392 I R F A Q M L E K V C V E T V E S G A M
1321 ccaaggacactggcggctgcattcacggcctcagcaatgtgaagctgaacggacttcc
412 T K D L A G C I H G L S N V K L N E H F
1381 tgaacaccacggacttcctcgacaccatcaagagaacctggacagagccctggcaaggc
432 L N T T D F L D T I K S N L D R A L G R
1441 agtaggggaggcgccaccatggctgcagtggagggccagggtggatggccgggtcc
452 Q *

1501 tcctgagcgcggcaggggtgagcctcacagccctctggaggccttctagggatg
1561 ttttttataagccagatgttttaaaagcatatgtgtttccctcatggtgacgtga
1621 ggcaggagcagtgcgtttacctcagccagtcaagatgtttgcatactgtatatttat
1681 tgcccttggaaacacatggccatatttagctactaaaaagcttccataaaaaaaaaaaa

4 / 12

Figure 3:

Isocitrate dehydrogenase anti sense fragment
(SEQ ID NO: 5)

5' TGCTCTGTGGCTAACCTCTGGTCCAGGCAAAATGGAAGCAATGGATTGGTGACGTCTCCTGT
CCTTCTGGTACATGCGGTAGTGACGGTTACAGTCCCGTGGCAGCCTCTGCTTCTACCGTCTGCCA
TCTGGACAAACCAGCACCGCTGGTCATCATGCCGAGAGAGCCATACCCCTGGGCCACAGAGTCCGACTGC
ACGTCAACCATCATAGTTTACAGGCCAGATGAAGCCTCCCTGTATCTCATAGCTGGGCCACCATG
TCGTCGATGAGCCTATGCTCATACCAGATCTTGAGCTCAAACGGACTTGTACTGCTGTATAT
ATCTCCTGAAAGATGTCTTAAAACGCCATCATATTCTCAGAATGGTTGGCTCAGATAC
AAAGGCCAACCTTAGACAGAGCCATTGGAAGGAACTGTGTGCAAAATCTCAATTGACTTATCTGA
TTATACATCCCCATGACAACACCACCTTCTCAAGTTATGTACCAGG' 3

Applicants: Paz Einat, et al.
U.S. Serial No.: 10/618,143
Filed: July 11, 2003
Title: ISOCITRATE DEHYDROGENASE AND USES THEREOF
REPLACEMENT SHEET

5/12

Figure 4:
IDH siRNA sequence
(SEQ ID NO:6)

5' AAUCGUGAUGCACCAACGAC '3

6/12

Figure 5A

Alignment between Isocitrate dehydrogenase 1 (XM_055088) and AS fragment

ICD	1	GGCGGCGAACGGGGCACGCCCTCGCACACCGAGAGATAATTGTGCTCCATGACCTT
IRT-4C1	1	-----
ICD	61	TATTTGGAAAGTCCTGCAGGGCTAAAATTGGCCTTGTCCCACCGAGTACACTCAGCAC
IRT-4C1	1	-----
ICD	121	TGTACTTTAACCGGATAAAACTGGGCTGTCTGGCAGGGATAAAACTACATTCAAGTTGAGT
IRT-4C1	1	-----
ICD	181	CTGCAAGACTGGGAGGAACGGGATAAGAAATCTATTCACTGTCAAGGTTATTGAA
IRT-4C1	1	-----
ICD	241	GTCAAAATGTCCAAAAAAATCAGTGGCGGTTCTGTGGTAGAGATGCAAGGAGATGAAATG
IRT-4C1	1	-----
ICD	301	ACACGAATCATTGGGAAATTGATTAAAGAGAAACTCATTTCCTACGTGGAATTGGAT
IRT-4C1	1	-----
ICD	361	CTACATAGCTATGATTAGGCATAGAGAACGATCGTGATGCCACCAACGACCAAGTCACCAAG
IRT-4C1	1	-----
ICD	421	GATGCTGCAGAACGCTATAAGAACGATAATGTTGGCGTCAAATGTGCCACTATCACTCCT
IRT-4C1	1	-----
ICD	481	GATGAGAACAGGGTTGAGGAGTTCAAGTTGAAACAAATGTGGAAATCACCAATGGCACC
IRT-4C1	1	-----
ICD	541	ATACGAAATATTCTGGGTGGCACGGTCTTCAGAGAACGCAATTATCTGCAAAATATCCCC
IRT-4C1	1	-----
ICD	601	CGGCTTGTGAGTGGATGGTAAACCTATCATCATAGTCGTATGCTTATGGGATCAA
IRT-4C1	1	-----
ICD	661	TACAGAGCAACTGATTGTTCTGGCCTGGAAAGTAGAGATAACCTACACACCA
IRT-4C1	1	-----
ICD	721	AGTGACGGAACCCAAAGGTGACATA[CCTGGTACATAACTTTGAAGAACGGTGGTGGTGT] [CCTGGTACATAAC-TTGAAGAACGGTGGTGGTGT]
IRT-4C1	1	-----
ICD	781	[GC]CATGGGGATGTATAATCAAGATAAGTCATTGAGATTTCACACAGTTCTTCCAA
IRT-4C1	34	[GT]CATGGGGATGTATAATCAAGATAAGTCATTGAGATTTCACACAGTTCTTCCAA
ICD	841	ATGGCTCTGTCTAAGGGTGGCCTTGTATCTGAGCACCAAAACACTATTCTGAAGAAA
IRT-4C1	94	ATGGCTCTGTCTAAGGGTGGCCTTGTATCTGAGCACCAAAACACCAATTCTGAAGAAA
ICD	901	TATGATGGCGTTTAAAGACATCTTCAGGAGATATATGACAAGCAGTACAAGTCCCAG
IRT-4C1	154	TATGATGGCGTTTAAAGACATCTTCAGGAGATATATGACAAGCAGTACAAGTCCCAG
ICD	961	TTTGAAGCTAAAAGATCTGGTATGAGCATAGGCTCATCGACGACATGGTGGCCCAAGCT
IRT-4C1	214	TTTGAAGCTAAAAGATCTGGTATGAGCATAGGCTCATCGACGACATGGTGGCCCAAGCT
ICD	1021	ATGAAATCAGAGGGAGGCTTCATCTGGGCCTGTAAAAACTATGATGGTGACGTGCAAGTCG
IRT-4C1	274	ATGAGATCAGAGGGAGGCTTCATCTGGGCCTGTAAAAACTATGATGGTGACGTGCAAGTCG
ICD	1081	GACTCTGTGGCCAAGGGTATGGCTCTCGGCATGATGACCAGCGTGTGGTTGTCCA
IRT-4C1	334	GACTCTGTGGCCAAGGGTATGGCTCTCGGCATGATGACCAGCGTGTGGTTGTCCA

7/12

Figure 5B

ICD	1141	GATGGCAAGACAGTAGAAGCAGAGGCTGCCACGGGACTGTAACCCGTCACTACCGCATG
IRT-4C1	394	GATGGCAAGACGGTAGAAGCAGAGGCTGCCACGGGACTGTAACCCGTCACTACCGCATG
ICD	1201	TACCAGAAAGGCACAGGGACAGTCCACCAATCCCATTGCTTCCATTTCGCTGGACCAGA
IRT-4C1	454	TACCAGAAAGGCACAGGGACAGTCCACCAATCCCATTGCTTCCATTTCGCTGGACCAGA
ICD	1261	GGGTTAGCCCACAGAGCAAAGCTTGATAACAATAAGAGCTTGCCTCTTGCAAATGCT
IRT-4C1	514	GGGTTAGCCCACAGAGCA-----
ICD	1321	TTGGAAGAAGTCTCTATTGAGACAATTGAGGCTGGCTTCATGACCAAGGACTTGGCTGCT
IRT-4C1	531	-----
ICD	1381	TGCATTAAGGTTACCCAATGTGCAACGTTCTGACTACTGAAATACATTGAGTTCATG
IRT-4C1	531	-----
ICD	1441	GATAAACTTGGAGAAAATTGAAGATCAAACACTAGCTCAGGCCAAACTTAAGTTCAACC
IRT-4C1	531	-----
ICD	1501	TGAGCTAAGAAGGATAATTGCTTTGGTAACTAGGTCTACAGGTTACATTTCGTTG
IRT-4C1	531	-----
ICD	1561	TTACACTCAAGGATAAAGGCAAAATCAATTGTAATTGTTAGAAGGCCAGAGTTATC
IRT-4C1	531	-----
ICD	1621	TTTCTATAAGTTACAGCCTTTCTTATATACAGTTATTGCCACCTTGTGAACAT
IRT-4C1	531	-----
ICD	1681	GGCAAGGGACTTTTACAATTTTATTCTAGTACCGCCTAGGAATTGGTT
IRT-4C1	531	-----
ICD	1741	AGTACTCATTGTATTCACTGTCACTTTCTCATGTTCTAATTATAATGACCAAAATC
IRT-4C1	531	-----
ICD	1801	AAGATTGCTAAAAGGTAAATGATGCCACAGTATTGCTCCCTAAATATGCATAAAGT
IRT-4C1	531	-----
ICD	1861	AGAAATTCACTGCCTCCCTCCTGTCCATGACCTGGGCACAGGAAAGTTCTGGTGTCA
IRT-4C1	531	-----
ICD	1921	TAGATATCCCGTTTGTGAGGTAGAGCTGTGCATTAAACTGCACATGACTGGAACGAAG
IRT-4C1	531	-----
ICD	1981	TAGGAGTGCAACTCAAATGTGTTGAAGATACTGCAGTCATTGTAAGACCTTGCTGA
IRT-4C1	531	-----
ICD	2041	ATGTTCCAATAGACTAAATACTGTTAGGCCGCAGGAGAGTTGGAATCCGGAATAAAT
IRT-4C1	531	-----
ICD	2101	ACTACCTGGAGGTTGTCCCTCTCCATTTCCTTCTCCTGGCCTGGCCTGAATAAT
IRT-4C1	531	-----
ICD	2161	TATACTACTCTAAATAGCATATTCATCCAAGTGAATAATGTAAGCTGAATCTTTTG
IRT-4C1	531	-----
ICD	2221	GACTTCTGCTGGCCTGTTATTCTTTATATAATGTGATTCTCAGAAATTGATATT
IRT-4C1	531	-----
ICD	2281	AAACACTATCTTATCTCTCCTG
IRT-4C1	531	-----

8/12

Figure 6
Alignment between IDH2 and IDH1 amino acid sequences

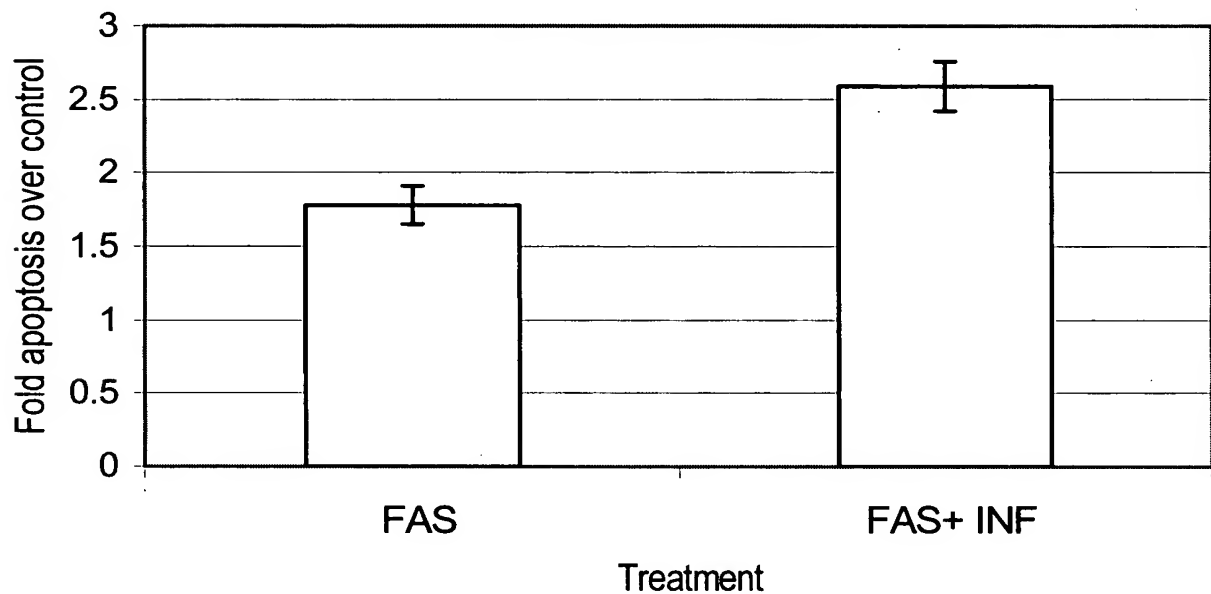
Score = 584 bits (1505), Expect = e-165
Identities = 281/397 (70%), Positives = 328/397 (81%), Gaps = 2/397 (0%)



IDH2: 50	VVEMDGDEMTRIIWQFIKEKILILPHVDIQLKYFDLGLPNRDQTDDQVTIDSALATQKYSV	109
	VVEM GDEMTRIIW+ IKEKLI P+V++ L +DLG+ NRD T+DQVT D+A A +K++V	
IDH1: 10	VVEMQGDEMTRIIWELIKEKLIFPYVELDLHSYDLGIENRDA	TNDQVTKDAAEAIKKHNV 69
IDH2: 110	AVKCATITPDEARVEEFKLKKMWKSPNGTIRNILGGTVFREPIICKNIPRLVPGWTKPIT	169
	VVKCATITPDE RVEEFKLK+MWKSPNGTIRNILGGTVFRE IICKNIPRLV GW KPI	
IDH1: 70	GVKCATITPDEKRVEEFKLQMKWKSPNGTIRNILGGTVFREAIICKNIPRLVSGWVKPII	129
IDH2: 170	IGRHAGHDQYKATDFVADRGTFKMFVFTPDKDGSVGKEWEVYNFP-AGGVGMGMYNTDESI	228
	IGRHA+GDQY+ATDFV G ++ +TP DG+ + V+NF GGV MGMYN D+SI	
IDH1: 130	IGRHAYGDQYRATDFVVPGPKVEITYTPSDGTQKVTLVHNFEEGGGVAMGMYNQDKSI	189
IDH2: 229	SGFAHSCFQYAIQKKWPLYMSTKNTILKAYDGRFKDIFQEIFDKHYKTDFDKNKIWYEHR	288
	FAHS FQ A+ K WPLY+STKNTILK YDGRFKDIFQEI+DK YK+ F+ KIWEHR	
IDH1: 190	EDFAHSSFQMALSKGWPLYLSTKNTILKKYDGRFKDIFQEIYDKQYKSQFEAQKIKIWYEHR	249
IDH2: 289	LIDDMVAQVLKSSGGFWACKNYDGDVQSDILAQGFGLGLMTSVLCPDGKTIEAEEAH	348
	LIDDMVAQ +KS GGF+WACKNYDGDVQSD +AQG+GSLG+MTSVLCPDGKT+EAEEAH	
IDH1: 250	LIDDMVAQAMKSEGGFIWACKNYDGDVQSDSVAQGYGSLGMMTSVLCPDGKTVEAEEAH	309
IDH2: 349	GTVTRHYREHQKGRPTSTNPIASIFAWTRGLEHRGKLDGNQDLIRFAQMILEKVCVETVES	408
	GTVTRHYR +QKG+ TSTNPIASIFAWTRGL HR KLD N++L FA LE+V +ET+E+	
IDH1: 310	GTVTRHYRMYQKGQETSTNPIASIFAWTRGLAHRAKLDNNKEAFFANALEEVSIETIEA	369
IDH2: 409	GAMTKDLAGCIHGLSNVKLNHEHFLNTTDFLDTIKSNL 445	
	G MTKDLA CI GL NV+ ++ +LNT +F+D + NL	
IDH1: 370	GFMTKDLAACIKGLPNVQRSD-YLNTFEFMDKLGEND	405

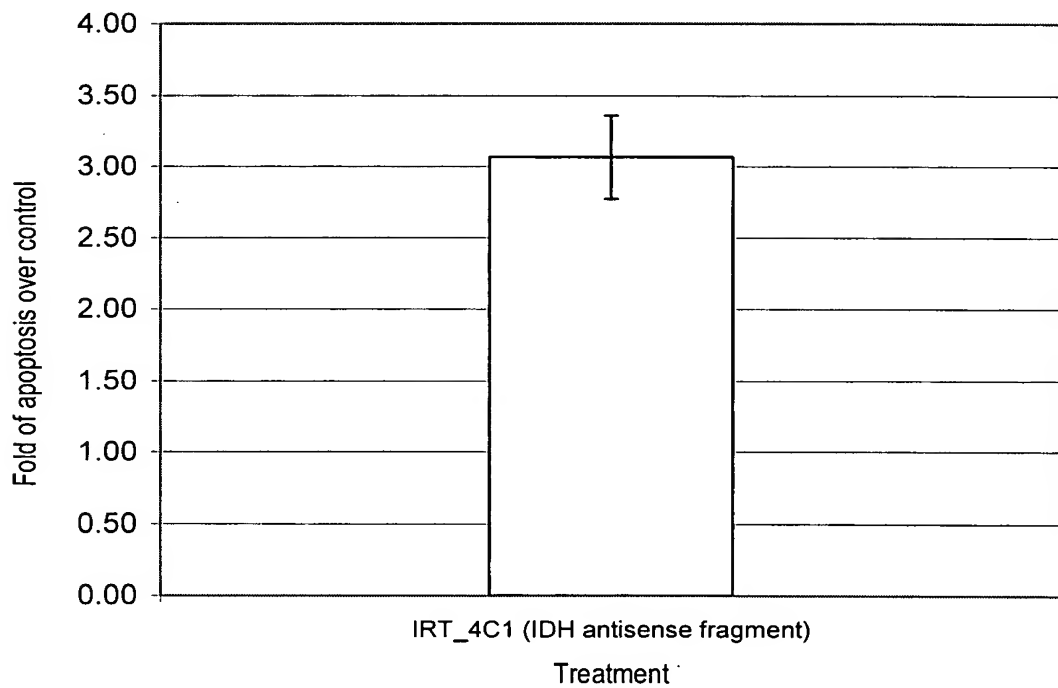
9 / 12

Figure 7



10/12

Figure 8



11/12

Figure 9A

Apoptosis protection

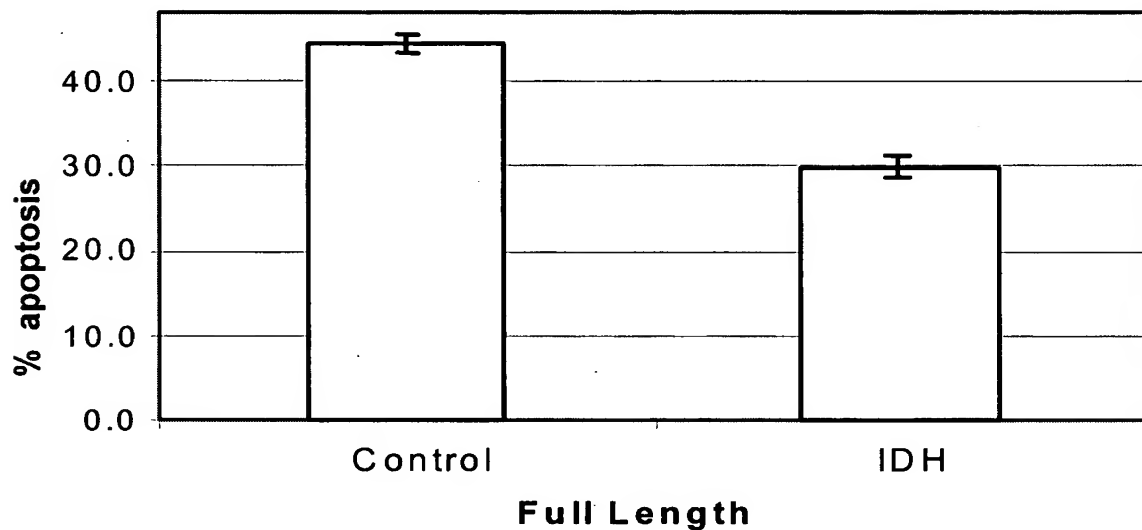
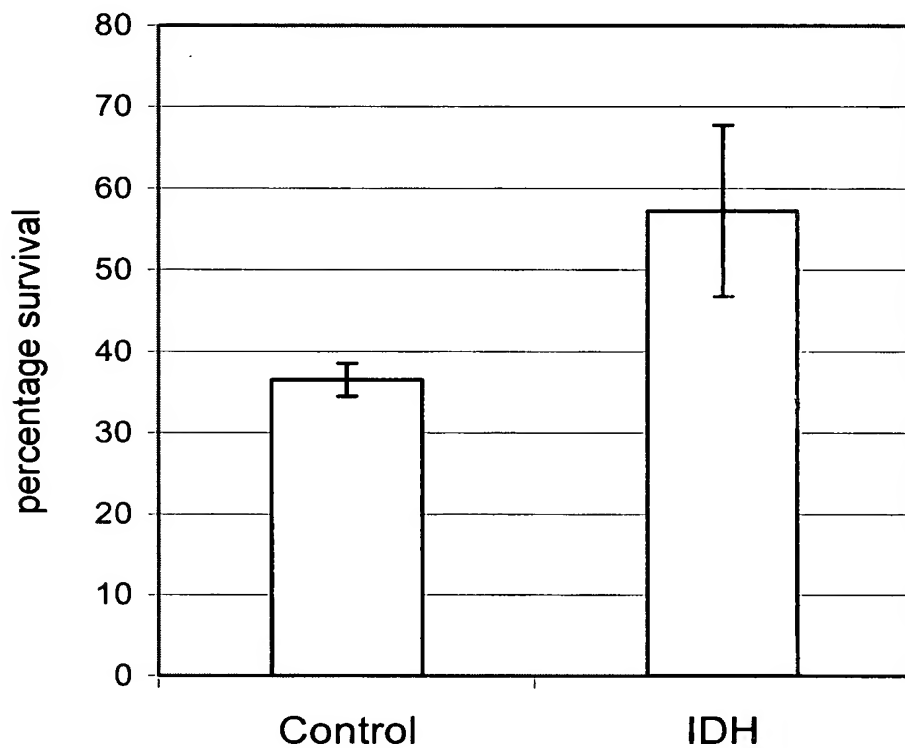


Figure 9B

Viability assay



12/12

Figure 10

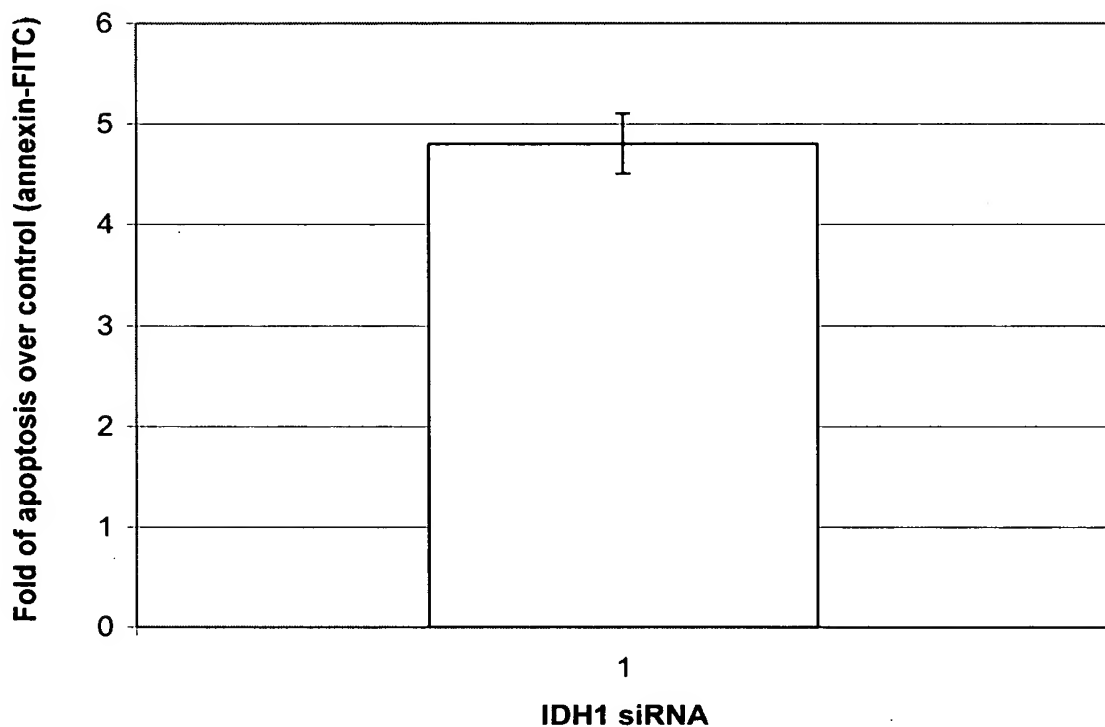
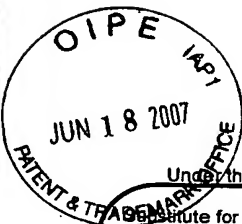


EXHIBIT C

Applicants: Paz Einat, et al.
U.S. Serial No.: 10/618,143
Filed: July 11, 2003



JUN 18 2007

U.S. Patent and Trademark Office; U.S. DEPARTMENT OF COMMERCE
Under the Paperwork Reduction Act of 1995, no persons are required to respond to a collection of information unless it contains a valid OMB control number.

PTO/SB/08B (04-07)

Approved for use through 09/30/2007. OMB 0651-0031
U.S. Patent and Trademark Office; U.S. DEPARTMENT OF COMMERCE
to a collection of information unless it contains a valid OMB control number.

INFORMATION DISCLOSURE STATEMENT BY APPLICANT

(Use as many sheets as necessary)

Sheet 1

1

Complete if Known	
Application Number	10/618,143
Filing Date	July 11, 2003
First Named Inventor	Paz Einat
Art Unit	1642
Examiner Name	Peter J. Reddig
Attorney Docket Number	67723-A/JPW/JW

NON PATENT LITERATURE DOCUMENTS

Examiner Signature		Date Considered	
*EXAMINER: Initial if reference considered, whether or not citation is made.			

EXAMINER: Initial if reference considered, whether or not citation is in conformance with MPEP 609. Draw line through citation if not in conformance and not considered. Include copy of this form with next communication to applicant.

1 Applicant's unique citation designation number (optional). **2** Applicant is to place a check mark here if English language Translation is attached.
This collection of information is required by 37 CFR 1.98. The information is required to obtain or retain a benefit by the public which is to file (and by the USPTO
to process) an application. Confidentiality is governed by 35 U.S.C. 122 and 37 CFR 1.14. This collection is estimated to take 2 hours to complete, including
gathering, preparing, and submitting the completed application form to the USPTO. Time will vary depending upon the individual case. Any comments on the
Trademark Office, P.O. Box 1450, Alexandria, VA 22313-1450. DO NOT SEND FEES OR COMPLETED FORMS TO THIS ADDRESS. SEND TO:
Commissioner for Patents, P.O. Box 1450, Alexandria, VA 22313-1450.

If you need assistance in completing the form, call 1-800-PTO-9199 (1-800-786-9199) and select option 2.

**Applicants: Paz Elnat, et al.
U.S. Serial No.: 10/618,143
Filed: July 11, 2003**

EXHIBIT 1

**Applicants: Paz Einat, et al.
U.S. Serial No.: 10/618,143
Filed: July 11, 2003**

REGULAR ARTICLE

Comparative proteomic analysis of esophageal squamous cell carcinoma

Yijun Qi^{1,2}, Jen-Fu Chiu^{3,4}, Lidong Wang¹, Dora L. W. Kwong⁵ and Qing-Yu He^{2,3}

¹ Laboratory for Cancer Research, College of Medicine, Zhengzhou University, Zhengzhou, China

² Department of Chemistry, University of Hong Kong, Hong Kong, China

³ Open Laboratory of Chemical Biology of the Institute of Molecular Technology for Drug Discovery and Synthesis, University of Hong Kong, Hong Kong, China

⁴ Institute of Molecular Biology, University of Hong Kong, Hong Kong, China

⁵ Department of Clinical Oncology, University of Hong Kong, Hong Kong, China

Ranking as the fourth commonest cancer, esophageal squamous cell carcinoma (ESCC) represents one of the leading causes of cancer death in China. One of the main reasons for the low survival rate is that neoplasms in esophagus are not detected until they have invaded into surrounding tissues or spread throughout the body at advanced stages. A better understanding of the malignant mechanism and early diagnosis are important for fighting ESCC. In this study, we used proteomics to analyze ESCC tissues, aiming at defining the proteomic features implicated in the multistage progression of esophageal carcinogenesis. Proteins that exhibited significantly different expressions were identified by peptide mass fingerprinting and validated by Western blotting and reverse transcriptase-polymerase chain reaction. The protein changes were then correlated to the different grades of disease differentiation. Compared to those in adjacent normal epithelia, the expression of 15 proteins including enolase, elongation factor Tu, isocitrate dehydrogenase, tubulin alpha-1 chain, tubulin beta-5 chain, actin (cytoplasmic 1), glyceraldehyde-3 phosphate dehydrogenase, tropomyosin isoform 4 (TPM4), prohibitin, peroxiredoxin 1 (PRX1), manganese-containing superoxide dismutase (MnSOD), neuronal protein, and transgelin was up-regulated; and the expression of five proteins including TPM1, squamous cell carcinoma antigen 1 (SCCA1), stratifin, peroxiredoxin 2 isoform a, and alpha B crystalline was down-regulated in cancer tissues with a statistical significance ($p < 0.05$). In addition, the differential expression of SCCA1, PRX1, MnSOD, TPM4, and prohibitin can be observed in precancerous lesions of ESCC. The expression of stratifin, prohibitin, and SCCA1 dropped with increasing dedifferentiation of ESCC. These data may suggest that these proteins contribute to the multistage process of carcinogenesis, tumor progression, and invasiveness of ESCC.

Received: September 6, 2004

Revised: November 4, 2004

Accepted: November 30, 2004

Keywords:

Esophageal cancer / Peroxiredoxin / Protein profiling / Squamous cell carcinoma antigen 1 / Transgelin / Tumor-associated proteins / Two-dimensional gel electrophoresis

Correspondence: Dr. Qing-Yu He, Department of Chemistry, University of Hong Kong, Pokfulam, Hong Kong, China
E-mail: qyhe@hku.hk
Fax: +852-2817-1006

Abbreviations: BCH, basal cell hyperplasia; CIS, carcinoma *in situ*; B-Cryst, alpha B crystalline; DYS, dysplasia; ESCC, esophageal squamous cell carcinoma; GAPDH, glyceraldehyde-3 phosphate dehydrogenase; MnSOD, manganese-containing superoxide dismutase; NADP, isocitrate dehydrogenase; PRX, peroxiredoxin; SCCA1, squamous cell carcinoma antigen 1; TPM, tropomyosin

1 Introduction

Esophageal squamous cell carcinoma (ESCC), the predominant histological subtype of esophageal cancer, is the fourth most common malignancy and still represents a great health concern in China. The incidence of ESCC is characterized by the striking geographic variation in incidence throughout the world [1, 2]. Linzhou (formerly Linjian) and Huixian, which geologically belong to Taihang Mountain region in northern China, have the highest incidence of ESCC in the

Applicants: Paz Einat, et al.
U.S. Serial No.: 10/818,143
Filed: July 11, 2003

www.proteomics-journal.de

Exhibit 1

world, with an incidence rate of approximately 150 per 100 000 population [1]. Most of the patients cannot survive more than 1 year after presenting at healthcare centers and the 5 year survival rate for ESCC remains as low as 10% or even less due to complications caused by the aberrant tumor growth in the esophagus, such as dysphagia, cachexia, etc. [3, 4]. One of the main reasons for the ominous phenomena is that neoplasms in esophagus are not detected until they have invaded the surrounding tissues or spread throughout the body at advanced stages. The early detection and diagnosis of esophageal malignancy is critical for its therapy and management.

A large number of epidemiological studies suggested that cigarette smoking, alcohol drinking, diets' deficiency in vitamins and/or protective antioxidants, and thermal injuries caused by hot food, intake of nitrosamine or moldy foodstuff which contain direct or indirect carcinogen have been closely correlated to the prevalence of esophageal cancer [5–7]. The etiological factors for ESCC, however, have yet to be clarified. Similar to other types of cancer, ESCC involves a multistage process, featuring a great diversity of genetic and epigenetic alterations. Although various molecular events and morphologic features have been found to closely correlate with malignancies of esophagus, the biomarkers for early detection and diagnosis with high specificity and sensitivity and indices for treatment and management of esophageal malignancy have not been identified.

Proteomics provides an effective approach to study disease pathogenesis by globally examining the different protein expressions due to malignant cell transformation in disease [8, 9]. Proteomic technology has been successfully applied to identify tumor-associated proteins in various cancers originating from different organs including liver [10], lung [11], prostate [12], breast [13], kidney [14], tongue [15], buccal mucosa [16], esophagus [17], bladder [18], and cholangiole [19]. In this study, we employed proteomics to analyze ESCC tumor specimens recruited from Linzhou, China, and to identify the proteins with significantly different expressions in cancer. The expression patterns of the proteins were then correlated to the different stages of malignancy and differentiation status of the disease. The present findings may shed light on the molecular characterization of esophageal cancer progression and may be informative for identifying biomarkers and therapeutic targets for ESCC.

2 Materials and methods

2.1 Tissue specimens

Tissues used in this experiment were obtained with the approval of the Committees for Ethical Review of Research involving Human Subjects at Zhengzhou University and the University of Hong Kong. A total of 17 human ESCC specimens were collected immediately after isolation of surgically resected tissues from patients in Linzhou in northern China.

The 17 cases included ten males and seven females with an average age of 60.2 ± 7.3 years. Tissue samples were snap-frozen in liquid nitrogen and then preserved in -80°C deep freezer or on dry ice for transfer before experiments. The histology for all 17 samples was confirmed by two independent histopathologist following fixation, embedding, sectioning, and H&E staining. All samples comprised more than 80% of target cells (normal epithelial cells, cells with various grades of disease, or cancer cells) without necrosis. These 17 cases were divided into two groups (Table 1). Group 1 contained 15 pairs of intramatched tissue specimens, i.e., tumor center tissues and matched normal esophageal epitheliums at least 5 cm distal from primary tumor mass of ESCC. Group 2 had two cases; each contained matched triplet samples including tumor and two pretumor lesions at different stages based on Lugol's staining (see below).

Table 1. Histopathological classification of ESCC specimens used for 2-D gel proteomic analysis

		Control and Pretumor			SCC			
		Normal	BCH	DYS	CIS	Well	Mod- erate	Poor
Group 1		15	—	—	—	1	5	9
Group 2	Case 23	—	—	1	1	—	1	—
	Case 28	—	1	1	—	—	1	—

Normal, normal esophageal epithelium; BCH, basal cell hyperplasia; DYS, dysplasia; CIS, carcinoma *in situ*; SCC, squamous cell carcinoma; Well, well-differentiated SCC; Moderate, moderately-differentiated SCC; Poor, poorly-differentiated SCC.

2.2 Preparation of tissue protein samples

Fresh frozen esophageal tissue samples (100–150 mg) were cut into small pieces, dissolved in lysis buffer at the ratio of 1 mg tissue per 2 μl lysis buffer (Reagent 3; Bio-Rad, Hercules, CA, USA) containing protease inhibitor cocktail (Sigma, St. Louis, MO, USA) 8340 and DNase I 1 U/mL and then homogenized for 5 min on ice with a minihomogenizer. The mixture was centrifuged at 13.2×1000 rpm at 4°C for 15 min to remove tissue and cell debris. The supernatant was taken as extracted proteins and the protein concentration was determined by the Bradford method with BSA as standard. Aliquots of protein samples were kept in -80°C deep-freezer until further use.

2.3 2-DE, silver staining, and image analysis

IEF was conducted using Amersham Biosciences IPGphor. IPG strips with a linear pH range of 3–10 were used for protein separation by following a protocol described previously [15, 20]. Proteins of 30–50 μg for analytical gels and 100–

200 µg for preparative gels were utilized for IEF and subsequent second dimensional separation. All samples were run at least in duplicate to guarantee reproducibility. Two good quality gels for each case were included into the subsequent image analysis. Silver staining was performed as previously described [15]. Images of 2-D gels were digitalized with ImageScanner (Amersham Biosciences). Image analyses were conducted with ImageMaster 2-D Elite software 4.01 (Amersham Biosciences) [15]. The normalized value for each protein spot volume was used for comparison. Only those spots that have statistical significance in differential expression were selected for further investigation.

2.4 In-gel digestion by trypsin

Spots of interest were cut out with a clean scalpel after the preparative gels were washed with Milli-Q water and transferred to a siliconized Eppendorf tube. Stained gel slabs were cut into 1 × 1 mm pieces and destained with 1 mL of 1:1 v/v mixture of 30 mM potassium ferricyanide and 100 mM sodium thiosulfate for 10 min and rinsed at least twice with Milli-Q water (1 mL for 5 min each) until the yellow color disappeared. The gel slabs were equilibrated with 0.5 mL of 50 mM NH₄HCO₃ for 10 min and then incubated with 0.5 mL of 1:1 mixture of 50 mM NH₄HCO₃ and 100% ACN for 30 min. Complete dehydration was achieved by incubation of gel slabs with 200 µL of 100% ACN and then gel pieces were dried in a SpeedVac for 20 min. For the in-gel digestion, the gel particles were rehydrated with a minimal volume of trypsin solution (10 µg/mL in 25 mM NH₄HCO₃) and incubated at 37°C overnight. The liquid fraction containing digested peptides was spotted onto a sample plate with equal amounts of matrix. Where necessary, the in-gel digests were extracted subsequently with 50 and 80% ACN, and then concentrated and desalting by ZipTip prior to applying on the sample plate [20].

2.5 MALDI-TOF MS and protein identification by peptide fingerprinting

A Voyage-DE STR MALDI-TOF mass spectrometer (Applied Biosystems, Foster City, CA, USA) was employed to obtain the peptide mass spectra with the following settings: reflector mode with 175 ns delay extraction time, 60–65% grid voltage, and 20 kV accelerating voltage. Laser shots of 250 per spectrum were used to acquire the spectra with mass range of 500–4000 Da. Mass calibration was performed by using autolytic fragment peaks of trypsin including 906.5049, 1153.5741, and 2163.0570 Da. Proteins were identified by peptide fingerprinting using MS-Fit to search the NCBI nr protein database (<http://prospector.ucsf.edu>). The criteria for database matching are ±25 ppm mass tolerance, at least four peptides matched, and corresponding molecular weights and pI values. The species of origin was restricted to *Homo sapiens*.

2.6 Western blotting

With reference to the verification of candidate proteins after peptide fingerprinting, the proteins of interest were selected for Western blotting to confirm the results of protein database searching. After 1- or 2-DE, proteins were transferred onto PVDF membranes (Amersham Biosciences) at 0.8 mA/cm² for 1 h. After blocking in 5% nonfat milk in TBS-T containing 0.1% Tween 20 (Sigma) at 4°C overnight with gentle rocking, membranes were probed with antibodies. Primary antibodies involved in this study include SCCA1 (SCCA1 8H11: sc-21767, Santa Cruz Biotechnology) diluted in 1:250, crystallin (SPA-223, Stressgen Biotechnologies) diluted in 1:2000, tropomyosin (TPM) (TM311, Sigma) diluted in 1:400. Membranes were incubated with corresponding primary antibody for various durations according to the specificity and sensitivity of antibody. After incubation with corresponding secondary antibodies, immunoblots were visualized with the ECL detection kit (Amersham Biosciences). For reprobing membranes with another antibody, the membranes were stripped with stripping buffer (glycine 3.75 g/L, SDS 2 g/L, pH 2.0) before blocking.

2.7 RNA isolation and RT-PCR

Trizol Reagent (GibcoBRL, Life technologies, USA) was used to isolate total RNA from frozen tissue samples according to protocol provided by supplier. Reverse transcription was performed using 3 µg of extracted total RNA mixed with reaction mixture in a final concentration of 0.5 mM dNTPs, 0.025 µg/µL oligo dT, 5 mM MgCl₂, 0.01 M DTT, 2 U/µL RNaseOUT™ inhibitor, and 2.5 U/µL SSI RT. The reaction was achieved by incubating each sample at 65°C for 5 min, placing on ice for 1 min, incubating at 42°C for 2 min, mixing with SSI RT followed by incubating at 42°C for 1 h, and incubating at 70°C for 15 min to stop reaction. Following RT, PCR was carried out in a reaction volume of 30 µL with final concentration of 1.5 mM MgCl₂, 0.1 mM dNTPs, 0.05 Taq DNA polymerase, and primer pair for SCCA1. Beta-actin was used for internal normalization. The primers used for SCCA1 and beta-actin are listed as follows. The reaction was initiated at 94°C for 10 min followed by 35 cycles at 94°C for 30 s, 55°C for 1 min, and 72°C for 1 min, and final extension at 72°C for 10 min.

SCCA1, sense primer 5'-GATTAAGAACGGTTCTCA
CTTGAA-3', antisense primer 5'-ATGTGGTATTGCTGC
CAAATTTACCTTCAGGAAT-3';

Beta-actin, sense primer, 5'-GTGGGGCGCCCCAGG
CACCA-3', antisense primer 5'-CTCCTTAATGTCACGCC
GATTC-3'.

2.8 Statistical analysis

Since there were only two cases in group 2, the statistical analysis was performed only for the 15 paired samples in group 1. Comparison was made between 15 normal samples

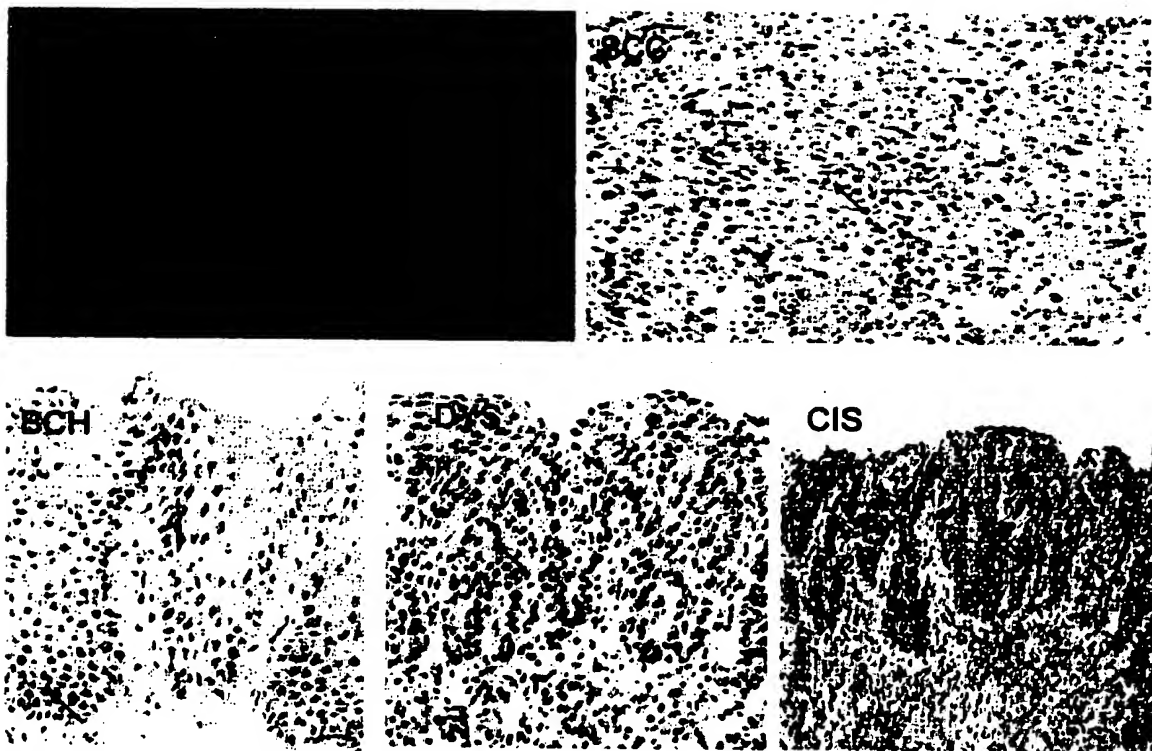


Figure 1. Representative histology of normal esophageal epithelium, BCH, DYS, CIS, and ESCC. Normal esophageal epithelium displays basal membrane, basal cells one to three layers (arrow head), suprabasal cells five to seven layers and superficial layers; BCH shows more than three layers of proliferation of basal cells (arrow head); DYS features loss of architectural orientation and comprises deranged cells with various size and shape and large deeply stained nuclei; CIS comprises malignant cells occupying the entire thickness of esophageal epithelium with intact basal membrane (dotted arrow); SCC comprises numerous malignant cells characterized by considerable pleomorphism and mitotic figures (arrow head).

and 15 SCC tumor samples regardless of their differentiation states. One-tailed Student's *t*-test was used for statistically analyzing the data extracted from comparison window of ImageMaster software that displayed the normalized volumes for each protein spot. A value of $p < 0.05$ was considered significant.

3 Results

3.1 Histological diagnosis of ESCC specimens

As shown in Fig. 1 and Table 1, two groups of tissue specimens were classified through detailed histological diagnosis. For group 1, the 15 matched SCC tumor tissues can be further characterized according to their differentiations into three subgroups, including one well-differentiated, five moderately-differentiated, and nine poorly-differentiated

SCC. The presence of ESCC and intramatched epithelium were confirmed by subsequent histological examination in which tissue section slides were stained with hematoxylin and eosin (Fig. 1). For group 2, Lugol's staining was performed before dissecting tissue specimens harboring precursor lesions of ESCC. Lugol's staining is a well-known procedure to screen out diseased conditions or precursor lesions of tumors originating from squamous epithelium, such as cervix of uterus and esophageal epithelium. Besides the cancer mass, adjacent nonstained and stained areas of esophageal epithelium in Lugol's staining were dissected. The nonstaining area of esophageal mucosae was considered to be precursor lesions for ESCC. As listed in group 2 in Table 1, case 23 comprised tissues of dysplasia (DYS), carcinoma *in situ* (CIS), and moderately-differentiated SCC; and case 29 consisted of tissues of basal cell hyperproliferation (BCH), DYS, and moderately-differentiated SCC, respectively (Fig. 1).

Table 2. Summary of PMF and statistical differences and *p*-values for the comparison between normal and cancer tissues

Spot no.	Protein ID (M/pI)	Experimental mass, kDa/pI	Peptides matched	Sequence coverage, %	Total mass error, ppm	MOWSE score	Differential ratio	<i>p</i> -value
304	Alpha enolase (47 kDa/8.98)	49/7.0	43	74	15.8	3.73e + 12	+1.8	8.181e - 05
309	Alpha enolase (47 kDa/8.98)	48/8.5	27	57	20	3.87e + 07	+1.7	0.0018
310	Alpha enolase (47 kDa/7.0)	49/8.5	44	67	17.4	1.74e + 13	+1.7	0.0001
344	Elongation factor Tu (P43) (48 kDa/8.31)	48/8.5	10	16	18.8	301	+2.0	0.0081
349	(NADP) cytoplasmic (48.7 kDa/8.53)	48/8.5	28	61	21.4	1.01e + 08	+2.1	0.0005
378	SCCA1 (45 kDa/8.3)	46/8.5	25	71	16.1	2.46e + 07	-2.5	8.474e - 05
386	TPM1 (34 kDa/4.8)	37/4.8	13	45	11	729	-1.7	0.0088
458	Tubulin alpha-1 chain and actin cytoplasmic 1 (50 kDa/4.94)	40/4.8	9	21	10.3	5.90e + 05	+4.0	4.384e - 06
484	Tubulin beta-5 chain (50 kDa/4.78)	50/4.8	9	28	25.4	1450	+5.2	0.0105
512	GAPDH (38 kDa/8.58)	35/8.0	8	18	16.1	234	+1.8	0.0028
534	TPM4 (27.5 kDa/4.8)	37/4.8	35	68	18.3	3.07e + 04	+2.7	0.0108
538	Gamma-actin (41.7 kDa/5.3)	39/8.0	10	24	13.2	1.06e + 04	+2.5	0.0001
539	GAPDH (38 kDa/8.6)	35/8.5	18	47	14.2	2.80e + 04	+5.3	8.882e - 05
546	GAPDH (38 kDa/8.6)	35/8.5	10	25	24.5	1005	+2.1	0.0133
550	TPM Isoform (28 kDa/4.8)	37/4.5	13	58	18.5	1383	+2.0	0.0028
588	Stratifin (28 kDa/4.7)	28/4.8	8	38	14.1	167	-1.5	0.0211
592	Prohibitin (30 kDa/8.6)	29/8.8	10	28	12.9	2131	+1.5	0.0078
701	Peroxiredoxin 1 (22 kDa/8.3)	24/8.0	17	51	18.4	7.73e + 08	+2.5	0.0003
708	MnSOD (23.7 kDa/8.9)	24/7.0	12	57	18.9	1.80e + 05	+1.7	0.0015
714	Peroxiredoxin 2 (22 kDa/5.7)	23/5.5	6	25	9.4	201	-1.5	0.0350
743	αB-Crys (21 kDa/8.7)	21/7.0	8	34	33.3	2530	-5.9	0.0020
785	Neuronal protein (31.5 kDa/8.1)	20/8.1	6	23	23.3	597	+4.2	9.278e - 05
806	Transgelin (SM22-alpha) (22.8 kDa/8.9)	20/8.5	18	49	12.7	6.13e + 04	+2.4	0.0024
808	Transgelin (SM22-alpha) (22.8 kDa/8.9)	20/8.8	16	63	18.8	1.55e + 04	+107	0.0008

3.2 2-DE protein separation and image analysis

2-DE using IPG (linear) ranging from 3 to 10 was performed to separate the proteins extracted from tumor and adjacent normal mucosa or precancerous tissue samples. Figure 2 shows one representative pair of proteome profilings for cancer (A) versus normal (B) tissue samples. There were around 942 spots unambiguously displayed on the 2-D gels according to the image analysis using software ImageMaster 2-D Elite. We found that most of the spots correlated well between 2-D maps of cancer and adjacent nontumor tissues. One-tailed Student's test was utilized to select the protein spots that showed significantly and consistently differences in expression through the intrapaired comparative analysis in ImageMaster. Twenty-four protein spots were revealed to have differential expressions between cancer tissues and adjacent normal esophageal epithelium with *p*-values less than 0.05 (Table 2). Among these protein spots, 19 were up-regulated and five were significantly down-regulated in ESCC tumor. The numbers denoted on the 2-DE maps in Fig. 2 represent these protein spots; the supposed positions of the spots absent or undetectable on one image but present on its counterpart gel are also indicated. The most substantial volume change is for spot 808, corresponding to a transgelin isoform, showing an averaged expression of 107-fold more in cancer tissues than in nontumor tissues. In

fact, for all the 17 paired cases, spot 808 was unequivocally displayed in 13 tumor cases but almost undetectable in the 2-DE maps of normal tissues or tissues with precursor lesions of ESCC (Fig. 3).

3.3 Protein identification by PMF

Protein spots with statistically consistent and significant differences in protein expression were excised, subjected to in-gel tryptic digestion, MALDI-TOF mass spectral measurements, and PMF to obtain protein IDs. Table 2 lists the identified protein IDs, together with corresponding spot numbers, molecular weights and pI values, peptides matched, sequence coverages, total mass errors, and MOWSE scores. For most of the protein database matching, reasonable sequence coverage, low mass errors, and high MOWSE scores were obtained. Proteins showing overexpressions in tumor are enolase, elongation factor Tu, isocitrate dehydrogenase (NADP), tubulin alpha-1 chain, tubulin beta-5 chain, actin (cytoplasmic 1), glyceraldehyde-3 phosphate dehydrogenase (GAPDH), TPM4, prohibitin, peroxiredoxin 1 (PRX1), manganese-containing superoxide dismutase (MnSOD), neuronal protein, and transgelin. Proteins that were down-regulated in tumor include TPM1, squamous cell carcinoma antigen 1 (SCCA1), stratifin, peroxiredoxin 2 isoform a (PRX2), and alpha B crystalline

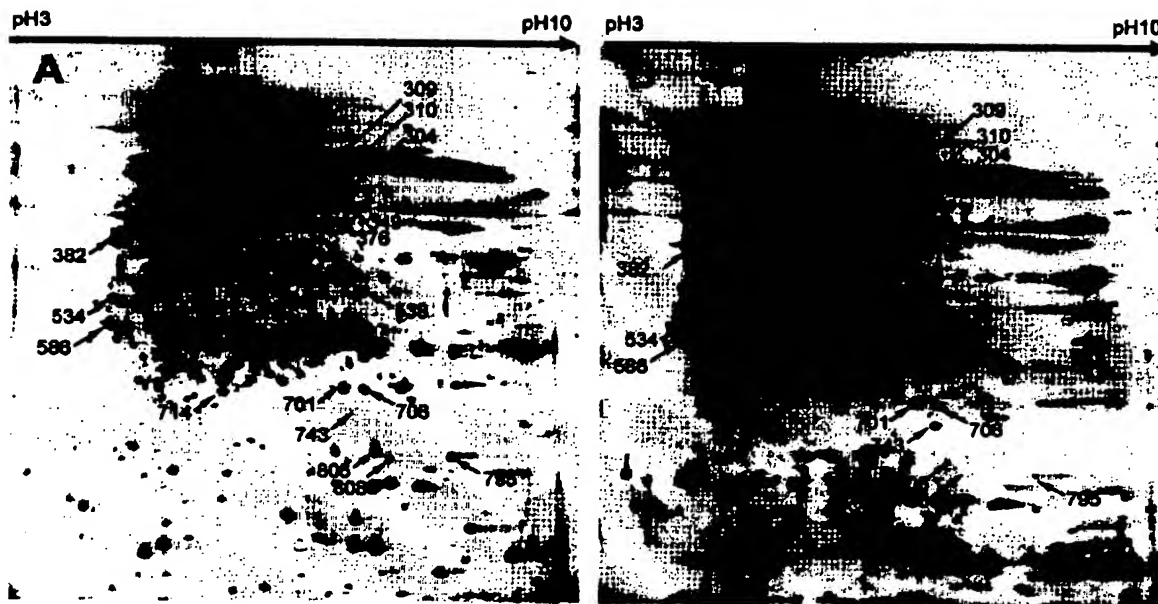


Figure 2. Representative images of 2-D gel for cancer (A) versus normal (B) tissue samples, respectively. Numbers indicated on map represents protein spots with differential expression.

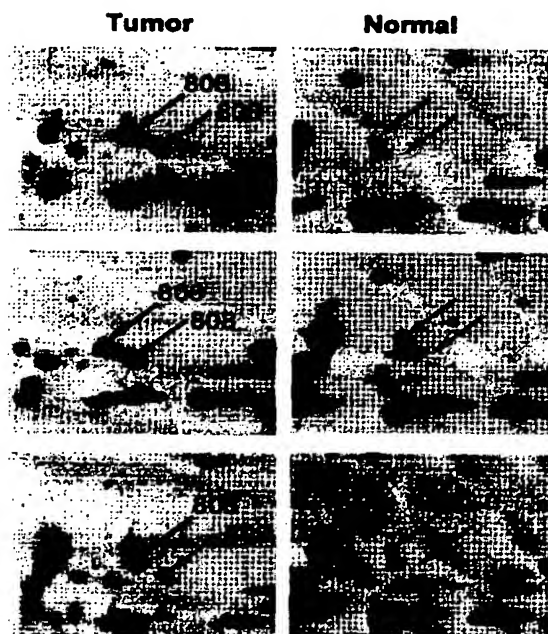


Figure 3. Cropped images of protein spots 806 and 808 (transgelin) in three pairs of ESCC samples. Transgelin isoform (808) presents exclusively on 2-D gels of cancer tissues.

(α -B-Cryst). Apparently different protein isoforms existed on proteomic profiling due to alternative splicing or PTM. Proteins displaying isoforms are transgelin, GAPDH, and alpha enolase.

3.4 Correlation of protein expression with histological grades of ESCC

The expression levels of the altered proteins were further correlated to the differentiation status of ESCC in group 1. As depicted in Fig. 4, we found that the expression changes for protein spots 376 (SCCA1), 586 (stratifin), and 592 (prohibitin) inversely correlate with differentiation grades of ESCC. The protein expression levels decreased with increasing dedifferentiation of ESCC from well-, to moderately-, to poorly-differentiated carcinoma.

Detailed protein expression analysis was also carried out for group 2 that contained two matched triplets of specimens from the same patients. Figure 5 shows consistent correlation or tendency relationships between lesion grades and protein expressions in the two cases. Clearly, expression levels of protein spots 534 (TPM4), 592 (prohibitin), 701 (PRX1), and 706 (MnSOD) linearly increased with progression of disease in the precancerous lesions from DYS to CIS (case 23) and from BCH to DYS (case 29) advancing to SCC. In addition, protein spot 376 (SCCA1) changed its expression level in reverse with the disease severity, consistent with the tendency found in group 1. A negative linear relationship

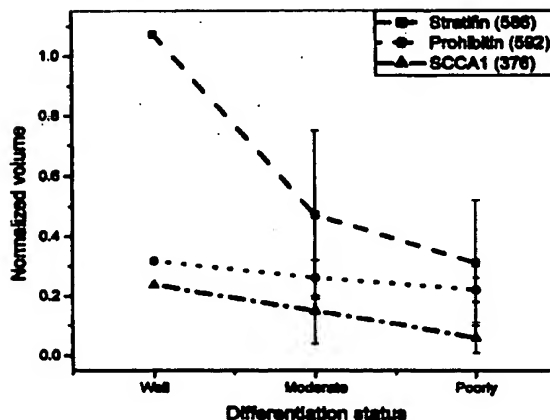


Figure 4. Correlation of protein expression with differentiation status of ESCC. Well, well-differentiated squamous cell carcinoma; moderate, moderately-differentiated squamous cell carcinoma; poorly, poorly-differentiated squamous cell carcinoma. Numbers in brackets are correlated protein spots on 2-D maps.

in terms of SCCA1 expression levels versus the general trend of disease aggravation can be derived. These protein alterations in expression reflect the dynamic molecular characterization of esophageal carcinogenesis.

3.5 Protein ID and expression confirmation by Western blotting

Western blotting was performed to verify three selected proteins, SCCA1, TPM1, and α B-Cryst, that may play functional roles in tumorigenesis. Figure 6 shows the 2-D Western blotting results with the corresponding silver staining 2-D gels side by side for the three proteins. Specific and positive immunochemical interactions occurred for the three proteins evaluated. Figure 7A displays the representative gels of 1-D Western blotting, confirming the decreased expressions of these three proteins in tumor tissues. Western blotting results shown in Fig. 7B exhibit the expression levels of SCCA1, the disease antigen, in the precancerous lesions in the specimens of group 2. In light with the data generated from the 2-D gel image analysis, SCCA1 expression levels in tissues decreased from DYS \rightarrow CIS \rightarrow SCC (case 23) and from BCH \rightarrow DYS \rightarrow SCC (case 29), reversely correlated to the aggravation states of the ESCC disease.

3.6 RT-PCR

To further verify the unusual expression of SCCA1 in transcription level, RT-PCR experiment was performed to compare the mRNA levels in tumor and nontumor tissues. Figure 8 shows the RT-PCR results for three representative pairs of the tissue samples. With the mRNA of beta-actin as internal control, the mRNA levels in nontumor tissues are

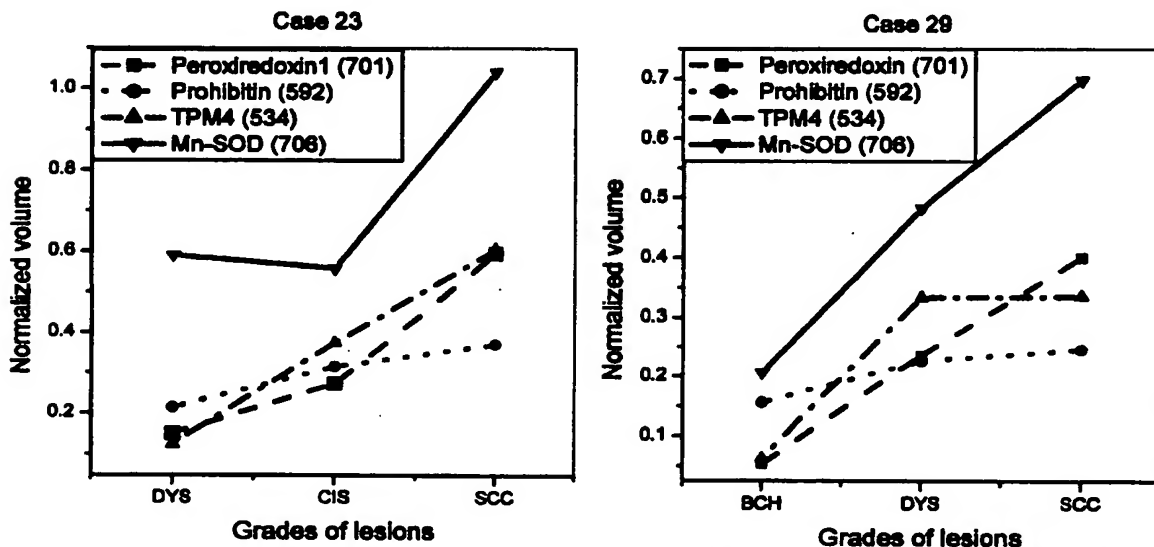


Figure 5. Expression of proteins, TPM4, prohibitin, PRX1, and MnSOD, in the two cases with precancerous lesions. Numbers in brackets represent protein spots on 2-D maps.

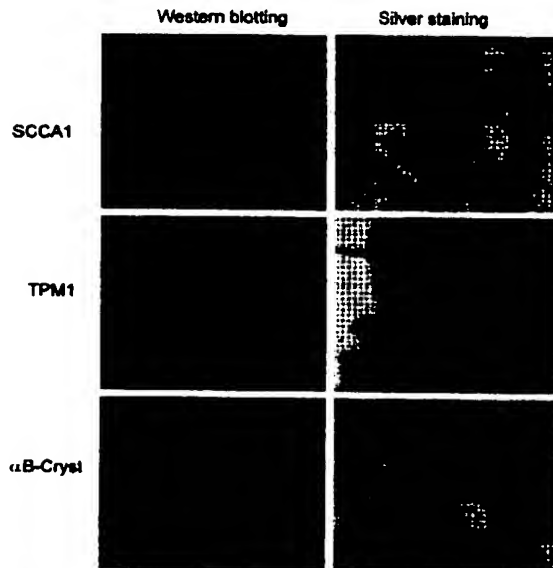


Figure 6. Protein confirmation for SCCA1, TPM1, and α B-Cryst by 2-D Western blotting.

obviously higher than those in tumor tissues, suggesting that the different expression of SCCA1 takes place at transcription stage.

4 Discussion

Although numerous studies in the genomic field have revealed a magnitude of changes occurring in the multistage pathogenesis of ESCC, including mutations of a variety of tumor suppressor genes and oncogenes, changes in transcription, proliferation-associated factors, and metastasis-related factors, these changes may not necessarily warrant subsequent corresponding alterations at the protein levels or functions [21–30]. Proteomics, which aims at characterizing the entire protein complement expressed in cells or tissues, provides complementary information and direct evidence to unravel tumor-specific molecular events during multistage carcinogenesis. In the present study, we used 2-DE based proteomics to examine the protein profiles of cancer tissues and the adjacent nontumor tissues freshly collected from Linzhou, the highest ESCC incident area in northern China, to identify proteins related to esophageal malignancy. A total of 20 proteins were uncovered with differential expressions in esophageal carcinogenesis, among which 15 were up-regulated and five were down-regulated.

The first intriguing identification is SCC antigen, SCCA1, which was found underexpressed in ESCC. Initially isolated from human cervical SCC tissue [31], SCCA belongs

to a serine protease inhibitor family (serpins). Serpins were found to be involved in a variety of biological functions, including fibrinolysis, coagulation, inflammation, tumor cell invasion, cellular differentiation, and apoptosis [32]. Biological studies have revealed that SCCA1 may function in cancer cells for tumor growth and in normal squamous epithelium for differentiation by inhibiting apoptosis [33]. The SCC antigen was found highly up-regulated in various SCC cancers including those in the uterine cervix, lung, head and neck, skin [33, 34] and recently in buccal mucosa [16]; this protein was therefore regarded as an SCC tumor marker. However, we observed that SCCA1 expression in ESCC cancer tissues was suppressed by 2.5-fold compared to adjacent normal tissues (Table 1). This unusual observation was further validated by Western blotting data, showing that the underexpression of SCCA1 not only takes place in tumor tissues in general (Fig. 7A) but also proceeds correlatively with malignant potential (Fig. 7B). A similar trend of SCCA1 down-regulation in ESCC tumor was found in RT-PCR experiment (Fig. 8), suggesting its firm occurrence in transcription level. This finding, although contradictory to the results from previous studies with other SCC cancers, implicates that the SCCA1 may have a unique function in esophagus SCC tumorigenesis. In addition, the decreased expression of SCCA1 can be linearly correlated to the differentiation progression of the disease in group 1 (Fig. 4). This finding is consistent with early observations that patients with well-differentiated esophageal tumors tended to have higher SCCA1 levels compared to those with poorly-differentiated tumors [35, 36]. Therefore, it is likely that SCCA1 is an indicator for the histological differentiation of the ESCC [37].

A group of cytoskeleton microfilament-associated proteins, including cytoplasmic actin, gamma-actin, transgelin, TPM1, TPM4, tubulin alpha-1 chain, and tubulin beta-5 chain, were found to express differentially between cancer and normal tissues. Actin network is essential for cellular functions such as motility, division and cell surface receptor movement, anchorage dependence, and contact inhibition. During malignant transformation, expression alterations in actin microfilament network and other actin-associated proteins always accompany morphological changes [38–41]. Previous studies have demonstrated that expression changes in cytoskeleton-associated proteins, including actin, TPM, gelsolin, caldesmon, and myosin light chain, have been implicated in transformed phenotypes [41].

TPM is a major structural component of cytoskeletal microfilament and multiple TPM isoforms have been reported in cultured nonmuscle cells. Interestingly, opposite expression regulations for different TPM isoforms have been often found in tumors, implying that these isoforms may have different functions in cell transformation. For example, underexpressions of high M_r TPM have been reported in various cancers such as oral tongue squamous cell carcinoma [15], breast [39, 42], and colon [42] cancers. Up-regulation of lower M_r TPM isoforms has been implicated to be

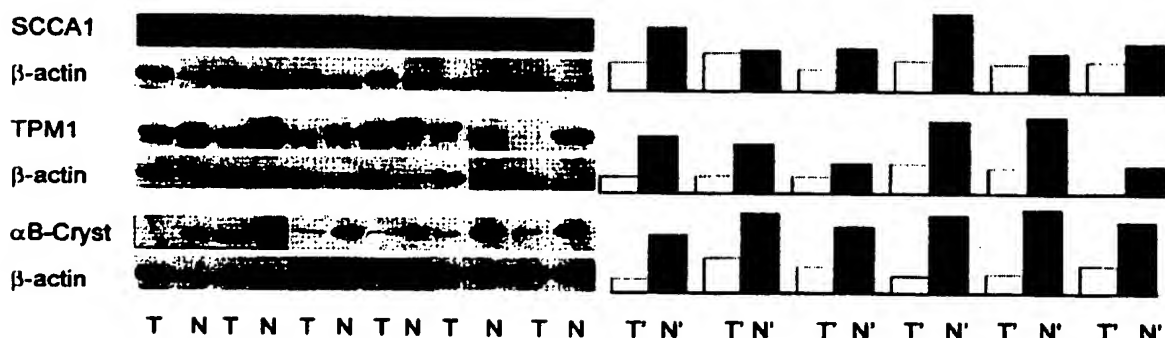
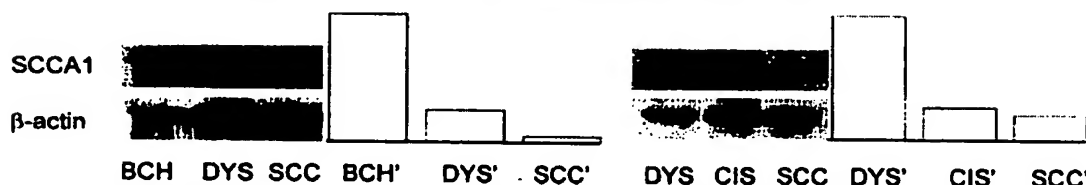
A: Western blots and normalized expression levels of proteins in Group 1**B: Western blots and normalized expression levels of SCCA1 in Group 2**

Figure 7. Western blots showing the protein expressions for SCCA1, TPM1, and α B-Cryst in tissues (T, tumor; N, normal) of group 1 (A); and SCCA1 expression in premalignant tissues of group 2 (B).

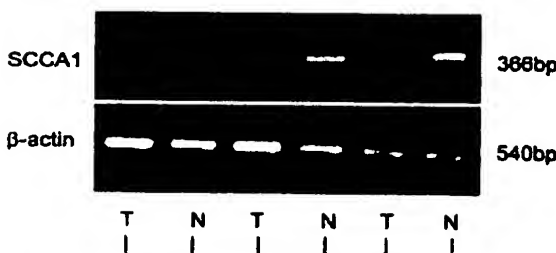


Figure 8. RT-PCR results for three representative pairs of tissue samples, showing that the mRNA level of SCCA1 is lower in tumor than in nontumor tissues. T, tumor; N, normal.

associated with metastatic potential of primary breast carcinoma [43], melanoma [44], and Lewis lung carcinoma [45]. Our current data validated the different regulations of TPM isoforms, with TPM1 being down-regulated and TPM4 being up-regulated significantly in ESCC tissues. The reverse regulation changes of TPM isoforms may cause an imbalance in normal phenotypes of epithelial microfilament and lead to malignant morphological changes of aberrant cells. These alterations may provide clues related to early detection and diagnosis and to the identification of therapeutic targets.

Transgelin is another cytoskeleton-associated protein related to cell transformation, division, adherence, and migration. Contradictory results concerning transgelin expression in tumors have been reported. For example, a proteomic analysis of matched normal ductal/lobular units and ductal carcinoma *in situ* (DCIS) of the human breast revealed that transgelin expression was at a higher level in normal ductal epithelial cells than in DCIS cells [13]. Transgelin gene expression at mRNA level was greatly reduced or lost in transformed and tumor cell lines [42]. However, a recent protein profile study discovered that transgelin was overexpressed in stomach cancer tissue [46]. Our current observation testified that transgelin expression was dramatically increased in ESCC, with a phenomenon that one distinct transgelin isoform (spot 808) presents exclusively in the cancer tissues (Fig. 3). Given the fact that esophagus and stomach are closely related in the digestive tract, ESCC and stomach cancer may be subjected to a similar stimulation in terms of cell malignant transformation related to transgelin expression. The underlying nature of transgelin functions in the tumorigenesis of esophagus and stomach warrants further investigation.

Accumulating evidence has indicated that intracellular redox state plays important roles in cellular signal transduction and gene expression [47]. Reactive oxygen species

(ROS), which are produced in cells during physiological processes in response to external stimuli, can affect intracellular redox state. At low levels, ROS modulate gene expression through modulating cellular redox state; at high levels, ROS are highly deleterious and potentially damage DNA, proteins, carbohydrates, and lipids. It has been suggested that ROS play roles in all stages of carcinogenesis, including initiation, promotion, and progression [48]. In order to protect themselves from oxidative radical stress, cells have developed defense systems that comprise proteins superoxide dismutases (SOD), catalase, glutathione peroxidases, and peroxiredoxins (PRX). The up-regulation of MnSOD and PRX1 in ESCC and their linear correlation with progression of disease from premalignant to invasive cancer (Fig. 5) reflect the cell defense effort in maintaining intracellular homeostasis. Similar observations have been found in other cancers including the overexpression of PRX in malignant mesothelioma [49], lung cancer [50], and oral cancer [51], and overexpression of MnSOD in human prostate cancer cell lines [52] and in buccal SCC [16]. Interestingly, a minor down-regulation of PRX2 isoform was detected in ESCC, suggesting that different PRX isoforms may have slightly different functions unique to the esophageal neoplasms.

α B-Crypt is a member of the small heat shock proteins (HSPs), which are ubiquitous chaperone molecules related to stresses. They can protect cells from damage through binding to partially denatured proteins, dissociating protein aggregates, modulating the correct folding, and cooperating in transporting newly synthesized polypeptides to the target organelles [53]. α B-Crypt was able to inhibit both the mitochondrial and death receptor apoptotic pathways through abolishing the autoproteolytic maturation of partially processed caspase-3 intermediate [54]. Intriguingly, while other HSPs were usually up-regulated in tumors, α B-Crypt was often down-regulated in various cancers [15, 55–59]. Our present data reinforced this observation with α B-Crypt being markedly suppressed in ESCC tissues. These results again revealed that α B-Crypt plays a role distinct from other HSPs in carcinogenesis and implicated that underexpression of α B-Crypt may be a general marker for various tumors.

Stratifin, also known as 14-3-3 σ or HME-1, was recently reported to be a candidate tumor suppressor gene that is transactivated by p53 in response to DNA damage and negatively regulates both G1/S and G2/M cell cycle progression [60, 61]. Overexpression of stratifin increased stabilization of p53 through blocking Mdm2-mediated p53 ubiquitination and enhanced oligomerization of p53, leading to an increase in p53 transcriptional activity [62]. Several studies have reported the potent role of stratifin in tumorigenesis of various organs, including prostate, urinary bladder, and breast [18, 63, 64]. In line with other published data, a small but significant underexpression of stratifin was found in cancer tissues in the present study, implicating its probable contribution to pathogenesis of esophageal neoplasms. Additionally, the stratifin expression was inversely correlated with

differentiation grade of ESCC (Fig. 4), indicating that malignant cells arising from esophageal epithelium may lose stratifin in progressive dedifferentiation.

Another potential tumor suppressor protein, prohibitin, was revealed to be differentially expressed between cancer tissue and adjacent normal epithelium. Interestingly, prohibitin expression positively correlated with the progression of precancerous lesions (Fig. 5) but inversely correlated with the differentiation grades of squamous cell carcinoma of esophagus (Fig. 4). This expression manner indicates that prohibitin may play different roles at different stages of esophageal tumorigenesis by acting on cell proliferation. One study using RNA interference to knock down prohibitin and using transient transfection to overexpress the protein demonstrated that cells with reduced prohibitin displayed a slight increase in the percentage of cell population in cell cycle, while cells with increased prohibitin showed a clear reduction in the percentage entering the cell cycle following dihydrotestosterone stimulation [65].

In summary, we used 2-D gel based proteomics to compare the protein profiles between ESCC tumor and matched surrounding tissues and to identify differently expressed proteins in the esophageal cancer. A number of tumor-associated proteins, including SCCA1, transgelin, TPM, prohibitin, PRX, α B-Crypt, and MnSOD, were detected with altered expressions, corresponding to a complicated multistep process involved in the initiation, formation, and progression of esophageal carcinoma. When the expressions of the proteins were correlated with the histological stages and differentiation status of ESCC tissues, linear progressions were found for most of the altered proteins, providing a rationale to understand the relationships between the functions of the tumor-associated proteins and the cell malignant transformation in esophageal tumorigenesis.

We wish to thank Yuan Zhou, Ruqing Jiao, Cynthia Y. H. Cheung and Guocui Yang for their skillful technical assistance for the completion of this study. We are also grateful to Professor Songliang Qiu for the review of histological classification of H&E tissue slides. We also thank Jillin Li for collecting samples, Zongmin Fan and Yanjie Li for helping prepare the tissue processing and photographs of H&E slides. This work was partially supported by Hong Kong Research Grants Council Grants HKU 7227/02M (to Q.Y.H.) and HKU 7218/02M (to J.F.C.), the Department of Chemistry, the Areas of Excellence scheme of Hong Kong University Grants Committee, and the National Outstanding Young Scientist Award 30025016 (China).

5 References

- [1] Yang, C. S., *Cancer Res.* 1990, 40, 2633–2644.
- [2] Li, J. Y., Liu, B. Q., Li, G. Y., Chen, Z. J. et al., *Int. J. Epidemiol.* 1991, 14, 127–133.

- [3] Clark, G. W., Roy, M. K., Corcoran, B. A., Carey, P. D., *Surg. Oncol.* 1996, 5, 149–164.
- [4] Oka, M., Yamamoto, K., Takahashi, M., Hakozaiki, M. et al., *Cancer Res.* 1996, 56, 2776–2780.
- [5] Hu, J., Nyren, O., Wolk, A., Bergstrom, R. et al., *Int. J. Cancer* 1994, 57, 38–46.
- [6] Cheng, K. K., Duffy, S. W., Day, N. E., Lam, T. H., *Int. J. Cancer* 1995, 60, 820–822.
- [7] Gardiou, A., Tzonou, A., Lipworth, L., Signoretto, L. B. et al., *Int. J. Cancer* 1996, 63, 295–299.
- [8] Hunt, D. F. J., *Proteome Res.* 2002, 1, 15–19.
- [9] He, Q. Y., Chiu, J. F., *J. Cell Biochem* 2003, 89, 888–898.
- [10] Kim, J., Kim, S. H., Lee, S. U., He, G. H. et al., *Electrophoresis* 2002, 23, 4142–4150.
- [11] Chen, G., Gharib, T. G., Huang, C. C., Thomas, D. G. et al., *Clin. Cancer Res.* 2002, 8, 2296–2308.
- [12] Meahan, K. L., Holland, J. W., Dawkins, H. J., *Prostate* 2002, 50, 54–63.
- [13] Wuifkuhle, J. D., Sgrol, D. C., Krutzsch, H., McLean, K. et al., *Cancer Res.* 2002, 62, 6740–6749.
- [14] Klade, C. S., Voss, T., Kryszak, E., Ahom, H. et al., *Proteomics* 2001, 1, 890–898.
- [15] He, Q. Y., Chen, J., Kung, H. F., Yuen, A. P. et al., *Proteomics* 2004, 4, 271–278.
- [16] Chen, J., He, Q. Y., Yuen, A. P., Chiu, J. F., *Proteomics* 2004, 4, 2465–2475.
- [17] Zhang, L. Y., Ying, W. T., Mao, Y. S., He, H. Z. et al., *World J. Gastroenterol.* 2003, 9, 650–654.
- [18] Moreira, J. M., Gromov, P., Celia, J. E., *Mol. Cell. Proteomics* 2004, 3, 410–419.
- [19] Sriwongsap, C., Sawangareettrakul, P., Subhasitanont, P., Panichakul, T. et al., *Proteomics* 2004, 4, 1135–1144.
- [20] He, Q. Y., Liu, G. K., Zhou, Y., Yuen, S. T. et al., *Proteomics* 2003, 3, 666–674.
- [21] Xing, E. P., Nie, Y., Wang, L. D., Yang, G. Y. et al., *Carcinogenesis* 1999, 20, 77–84.
- [22] Cai, Y. C., Yang, G. Y., Nie, Y., Wang, L. D. et al., *Carcinogenesis* 2000, 21, 603–609.
- [23] Xing, E. P., Nie, Y., Song, Y., Yang, G. Y. et al., *Clin. Cancer Res.* 1999, 5, 2704–2713.
- [24] Shi, S. T., Yang, G. Y., Wang, L. D., Xue, Z. et al., *Carcinogenesis* 1999, 20, 591–597.
- [25] Montesano, R., Hollstein, M., Hainsaut, P., *Int. J. Cancer* 1996, 69, 225–235.
- [26] Yang, G., Zhang, Z., Liao, J., Seril, D. et al., *Int. J. Cancer* 1997, 72, 748–751.
- [27] Shimoyama, S., Konishi, T., Kawahara, M., Aoki, F. et al., *Hepatogastroenterology* 1998, 45, 1497–1504.
- [28] Shibagaki, I., Shimada, Y., Wagata, T., Ikanaga, M. et al., *Cancer Res.* 1994, 54, 2998–3000.
- [29] Yu, C. C., Filipe, M. I., *Histochem. J.* 1993, 25, 843–853.
- [30] Gerdes, J., Schwab, U., Lemke, H., Stein, H., *Int. J. Cancer* 1983, 31, 19–20.
- [31] Kato, H., Morofka, H., Aramaki, S., Torigoe, T., *Cell Mol. Biol. Incl. Cytol. Enzymol.* 1979, 25, 51–56.
- [32] Silverman, G. A., Bird, P. I., Carroll, R. W., Church, F. C. et al., *J. Biol. Chem.* 2001, 276, 33293–33296.
- [33] Suminami, Y., Nawata, S., Kato, H., *Tumour Biol.* 1998, 19, 489–493.
- [34] Torre, G. C., *Tumour Biol.* 1998, 19, 517–526.
- [35] Gion, M., Milne, R., Dittadi, R., Bruscagnin, G. et al. In: Kato, H., de Brujin, H. W. A., Ebert, W., Herberman, R. B., Johnson, J. T. (Eds.), *SCC Antigen in the Management of Squamous Cell Carcinoma*, Excerpta Medica, Princeton 1987, pp. 130–141.
- [36] Hirata, S., Yamazaki, K., Yokoyama, Y., Ueda, M. et al., *Nippon Gekka Zasshi* 1989, 90, 267–272.
- [37] Matsuda, H., Mori, M., Tsujitani, S., Ohno, S. et al., *Cancer* 1990, 65, 2261–2265.
- [38] Shapland, C., Hsuan, J. J., Totty, N. F., Lawson, D., *J. Cell Biol.* 1993, 121, 1065–1073.
- [39] Raval, G. N., Bharadwaj, S., Levine, E. A., Willingham, M. C. et al., *Oncogene* 2003, 22, 6194–6203.
- [40] Bharadwaj, S., Prasad, G. L., *Cancer Lett.* 2002, 183, 205–213.
- [41] Button, E., Shapland, C., Lawson, D., *Cell Motil. Cytoskeleton* 1996, 30, 247–251.
- [42] Shields, J. M., Rogers-Graham, K., Der, C. J., *J. Biol. Chem.* 2002, 277, 9790–9799.
- [43] Frenzen, B., Linder, S., Uryu, K., Alsalha, A. A. et al., *Br. J. Cancer* 1996, 73, 909–913.
- [44] Miyado, K., Kimura, M., Taniguchi, S., *Biochem. Biophys. Res. Commun.* 1998, 228, 427–435.
- [45] Tabanaga, K., Nakamura, Y., Sekiyaama, S., *Mol. Cell Biol.* 1988, 8, 3834–3837.
- [46] Ryu, J. W., Kim, H. J., Lee, Y. S., Myong, N. H. et al., *J. Korean Med. Sci.* 2003, 18, 505–509.
- [47] Kamata, H., Hirata, H., *Cell Signal.* 1999, 11, 1–14.
- [48] Kleunig, J. E., Xu, Y., Isenberg, J. S., Bachowski, S. et al., *Environ. Health Perspect.* 1998, 106 (Suppl. 1), 289–295.
- [49] Kinnula, V. L., Lehtonen, S., Sormunen, R., Kaarteenaho-Wilk, R. et al., *J. Pathol.* 2002, 196, 318–323.
- [50] Chang, J. W., Jeon, H. B., Lee, J. H., Yoo, J. S. et al., *Biochem. Biophys. Res. Commun.* 2001, 289, 507–512.
- [51] Yanagawa, T., Iwasa, S., Ishii, T., Tabuchi, K. et al., *Cancer Lett.* 2000, 156, 27–38.
- [52] Zhong, W., Yan, T., Webber, M. M., Oberley, T. D., *Antioxid. Redox Signal.* 2004, 6, 513–522.
- [53] Hard, F. U., *Nature* 1998, 391, 571–579.
- [54] Kamradt, M. C., Chen, F., Sam, S., Cryns, V. L., *J. Biol. Chem.* 2002, 277, 38731–38738.
- [55] Kato, K., Ito, H., Hasagawa, K., Inaguma, Y. et al., *J. Neurochem.* 1996, 68, 946–950.
- [56] Kato, M., Herz, F., Briljall, D., Kato, S., *Experientia* 1994, 50, 479–482.
- [57] Klemenz, R., Scheier, B., Muller, A., Steiger, R. et al., *Verh. Dtsch. Ges. Pathol.* 1994, 78, 34–35.
- [58] Hitotsumatsu, T., Iwaid, T., Fukui, M., Tateishi, J., *Cancer* 1996, 77, 362–361.
- [59] Takashi, M., Sakata, T., Ohmura, M., Kato, K., *Urol. Res.* 1997, 25, 173–177.
- [60] Hermeking, H., Lengauer, C., Polyak, K., He, T. C. et al., *Mol. Cell* 1997, 1, 3–11.
- [61] Laronga, C., Yang, H. Y., Neal, C., Lee, M. H., *J. Biol. Chem.* 2000, 275, 23106–23112.

- [62] Yang, H. Y., Wen, Y. Y., Chen, C. H., Lozano, G. et al., *Mol. Cell Biol.* 2003, 23, 7096–7107.
- [63] Cheng, L., Pan, C. X., Zhang, J. T., Zhang, S. et al., *Clin. Cancer Res.* 2004, 10, 3064–3068.
- [64] Simpson, P. T., Gale, T., Reis-Filho, J. S., Jones, C. et al., *J. Pathol.* 2004, 202, 274–285.
- [65] Gamble, S. C., Odontiodis, M., Waxman, J., Westbrook, J. A. et al., *Oncogene* 2004, 23, 2996–3004.

EXHIBIT 2

**Applicants: Paz Einat, et al.
U.S. Serial No.: 10/618,143
Filed: July 11, 2003**

Novel Molecular Signalling and Classification of Human Clinically Nonfunctional Pituitary Adenomas Identified by Gene Expression Profiling and Proteomic Analyses

Carlos S. Moreno,¹ Chheng-Orn Evans,¹ Xianquan Zhan,³ Mammerhi Okor,⁶ Dominic M. Desiderio,^{1,4,5} and Nelson M. Oyesiku²

¹Department of Pathology and Laboratory Medicine and Winship Cancer Institute and ²Department of Neurosurgery and Laboratory of Molecular Neurosurgery and Biotechnology, Emory University School of Medicine, Atlanta, Georgia; ³Charles B. Stout Neuroscience Mass Spectrometry Laboratory and Departments of ⁴Neurology and ⁵Molecular Sciences, University of Tennessee, Health Science Center, and University of Tennessee Cancer Institute, Tennessee; and ⁶Department of Neurosurgery, University of Alabama School of Medicine, Birmingham, Alabama

Abstract

Pituitary adenomas comprise 10% of intracranial tumors and occur in about 20% of the population. They cause significant morbidity by compression of regional structures or the inappropriate expression of pituitary hormones. Their molecular pathogenesis is unclear, and the current classification of clinically nonfunctional tumors does not reflect any molecular distinctions between the subtypes. To further elucidate the molecular changes that contribute to the development of these tumors and reclassify them according to the molecular basis, we investigated 11 nonfunctional pituitary adenomas and eight normal pituitary glands, using 33 oligonucleotide GeneChip microarrays. We validated microarray results with the reverse transcription real-time quantitative PCR, using a larger number of nonfunctional adenomas. We also used proteomic analysis to examine protein expression in these nonfunctional adenomas. Microarray analysis identified significant increases in the expression of 115 genes and decreases in 169 genes, whereas proteomic analysis identified 21 up-regulated and 29 down-regulated proteins. We observed changes in expression of SFRP1, TLE2, PITX2, NOTCH3, and DLK1, suggesting that the developmental Wnt and Notch pathways are activated and important for the progression of nonfunctional pituitary adenomas. We further analyzed gene expression profiles of all nonfunctional pituitary subtypes to each other and identified genes that were affected uniquely in each subtype. These results show distinct gene and protein expression patterns in adenomas, provide new insight into the pathogenesis and molecular classification of nonfunctional pituitary adenomas, and suggest that therapeutic targeting of the Notch pathway could be effective for these tumors. (Cancer Res 2005; 65(22): 10214-22)

Introduction

Pituitary adenomas account for ~ 10% of intracranial tumors and occur in about 20% of the population. They cause significant

morbidity by compression of regional structures and the inappropriate expression of pituitary hormones (1, 2). Nonfunctional pituitary adenomas, so-called because they do not cause clinical hormone hypersecretion (2-5), account for ~ 30% of pituitary tumors (3). The nonfunctional tumors are uniquely heterogeneous (Table 1), typically quite large, and cause hypopituitarism or blindness from regional compression (1).

Despite the lack of clinical hormone hypersecretion, immunohistochemical staining for hormones reveals evidence for hormone expression in up to 79% of these tumors, which we will refer to as immunohistochemically positive nonfunctional (NF⁺) tumors. The remainder are negative for hormone expression (2, 5) and will be referred to as immunohistochemically negative nonfunctional (NF⁻) tumors. However, current pathologic classification (Table 1) of these tumors has no molecular basis, and surprisingly, is based only on anterior pituitary hormone histochemistry for hormones, or on electron microscopy, which is of limited use.

Unlike the functional pituitary tumors, there is no available effective medical therapy for the nonfunctional tumors, and only a better understanding of the molecular biology of these tumors will provide needed medical treatment options.

Although pituitary tumors are mostly benign, 5% to 35% of them are locally invasive. A small number exhibit a more aggressive course, infiltrate dura, bone and sinuses and are highly aggressive. A significantly smaller number are truly malignant; that is, they metastasize outside the central nervous system. It is not known what molecular profiles result in local invasion or presage a more aggressive course.

Molecular genetic studies have shown that these tumors are monoclonal in origin (6, 7). A minority is part of an autosomal-dominant syndrome, multiple endocrine neoplasia type 1 (MEN1), which is associated with mutations in the *MEN1* tumor suppressor gene. Others are associated with loss of heterozygosity on the 11q13 chromosome (2, 8-10). A dominant mutation occurs in the *Gαs* gene in ~ 30% of somatotrophinomas, but this mutation is rare in other pituitary tumors (2, 11, 12). In nonfunctional tumors, reduced levels of expression of the retinoid X receptor, estrogen receptor, and thyroid hormone receptor have been found and may contribute to abnormal thyroid hormone regulation of α-subunit production in these tumors. However, the significance of these data to pituitary tumorigenesis is unknown (13). The epidermal growth factor receptor (EGFR) is overexpressed in 80% of nonfunctional adenomas and is virtually undetectable in functional adenomas. *In vitro*, nonfunctional tumors in culture proliferate in response to EGF administration and up-regulate EGFR mRNA (14). In addition, we

Note: Supplementary data for this article are available at Cancer Research Online (<http://cancerres.aacrjournals.org/>).

The laboratory of D.M. Desiderio contributed the proteomic data, and the laboratory of N.M. Oyesiku contributed the microarray and reverse transcriptase real-time quantitative PCR data to this study.

Requests for reprints: Nelson M. Oyesiku, Department of Neurosurgery, Emory University School of Medicine, 1365-B Clifton Road Northeast, Suite 6400, Atlanta, GA 30322. Phone: 404-778-4737; Fax: 404-778-4472; E-mail: noyesik@emory.edu.

©2005 American Association for Cancer Research.
doi:10.1158/0008-5472.CAN-05-0884

Table 1. Classification of nonfunctional pituitary adenomas by cell of origin

Cell type	Hormone expression	% Nonfunctional tumors
Null cell	None	17
Oncocytoma	None	6
Silent corticotroph	ACTH	8
Silent somatotroph	GH	3
Gonadotrophs	Intact LH/FSH or subunits	40-79

recently found that the folate receptor is overexpressed in nonfunctional pituitary adenomas (15, 16).

To further elucidate the molecular changes that contribute to the development of these tumors and reclassify them according to the molecular basis, we used microarray analysis to elucidate the gene expression profile of 11 nonfunctional pituitary adenomas compared with eight normal pituitary glands.

We verified the gene expression changes of four genes that were detected by microarray analysis in 23 nonfunctional pituitary tumors and eight normal pituitary glands by reverse transcription real-time quantitative PCR (RT-qPCR). To complement and extend the expression profiling data, a comparative proteomics system based upon two-dimensional PAGE and mass spectrometry (MS) were used to characterize each differentially expressed protein in the same pituitary adenoma tissues.

Materials and Methods

Patients and tumor characterization. Sporadic pituitary adenomas were obtained from patients at the Emory University Hospital during transsphenoidal surgery (Supplementary Table 1). Informed consent for inclusion in this study was obtained. Pituitary adenomas are anatomically and pathologically distinct from the normal anterior lobe, making them easy to dissect under the surgical microscope. All tumors were microdissected and removed using the surgical microscope, rinsed in sterile saline, snap-frozen in liquid nitrogen, and stored (-80°C) for molecular analysis and proteomics. Each tumor fragment was then confirmed independently by a neuropathologist as being homogenous and unadulterated by histology and immunohistochemistry before molecular analysis.

Eight normal pituitary glands obtained from the National Hormone and Pituitary Program, National Institute of Diabetes and Digestive and Kidney Diseases (Bethesda, MD; $n = 3$) and from the National Disease Research Interchange (Philadelphia, PA; $n = 5$) were used as controls for microarray and RT-qPCR analyses. Eight normal pituitary glands obtained from the Memphis Regional Medical Center ($n = 7$) and the National Disease Research Interchange ($n = 1$) were used as controls in proteomics.

Synthesis of biotin-labeled cRNA and microarray hybridization. Total RNA extraction was previously described (15, 16). Briefly, total RNA (100 μg) was purified, using the RNeasy Mini Kit (Qiagen, Inc., Valencia, CA) with minor modifications. Total RNA was eluted twice with 50 μL of 65°C DEPC-treated water. Double-strand cDNA was synthesized from 25 μg total RNA with the Superscript II (Invitrogen, Carlsbad, CA) and a T7-(dT)24 oligomer then purified by phase-lock gel (Eppendorf, Westbury, NY) with phenol/chloroform extraction. Biotin-labeled cRNA was produced with Enzo BioArray High Yield RNA Transcription Labeling kit according to the manufacturer's instructions. The biotinylated cRNA was fragmented to 50 to 200 nucleotides by heating (94°C for 35 minutes) and chilled on ice.

For microarray analysis, three normal pituitary glands and 11 nonfunctional pituitary adenomas were analyzed using HG-U95Av2 GeneChips (Affymetrix, Santa Clara, CA) at the Emory/Veterans' Administration Medical Center (Atlanta, GA). All samples were analyzed in duplicate, starting from

the extraction of total RNA, GeneChip hybridization, washing, scanning, and data analysis. Five additional normal pituitary glands were analyzed once using the same chips, HG-U95Av2 GeneChips at the Moffit Comprehensive Cancer Center, University of South Florida (Tampa, FL).

Data analysis. Gene expression data from 12,625 probe sets on the HG-U95Av2 GeneChips were normalized, using GCRMA normalization with GeneTraffic Software (Iobion, La Jolla, CA). After data normalization, genes with uniformly low expression were removed from consideration, leaving 7,241 probe sets for analysis using significance analysis of microarrays (SAM) software (17). The following are the relevant variables for the SAM analysis: imputation engine, 10-nearest neighbor; number of permutations, 500; RNG seed, 1234567; delta, 1.063; fold change, 2.0. Normalized expression data from the 297 significant probe sets were analyzed by a two-dimensional hierarchical clustering, using Spotfire DecisionSite 8.1 software. Data was clustered using unweighted averages and ordered using average Euclidian distance.

For K-nearest neighbor (KNN) prediction, the normalized RT-qPCR data was analyzed with GenePattern software (<http://www.broad.mit.edu/cancer/software/genepattern/>), and both the KNN cross-validation and class prediction modules were used (KNN = 3). For these analyses, the four genes (or features) that were included were NADP-dependent isocitrate dehydrogenase (*IDH1*), paired-like homeodomain transcription factor 2 (*PTX2*), Notch homologue 3 (*NOTCH3*), and delta-like 1 homologue (*Drosophila*, *DLK1*).

To identify genes uniquely altered in tumor subtypes, SAM analysis was done with both the normal samples and other tumor subtypes as the control group, and the subtype of interest as the experimental group. Analyses were done with 500 permutations, fold change of 2.0, and false discovery rate (FDR) < 1%.

Reverse transcriptase real-time quantitative PCR. RT-qPCR was done as described (15, 16) on four gene transcripts in 23 nonfunctional pituitary adenomas and eight normal pituitary glands in a blinded fashion. Primers were selected using Primer Express software, version 2.0 (PE Applied Biosystems, Foster City, CA). BLASTed against all *Homo sapiens* gene sequences in Genbank for selectivity. The following are the primers of these genes:

	Forward primer	Reverse primer
<i>IDH1</i>	CACTACCGCATGT ACCAGAAAGG	TCTGGTCAGGC AAAAATGG
<i>PTX2</i>	GCCGGGATCGTAG GACCTT	GTGCCAACGACC TTCTAGCA
<i>NOTCH3</i>	TCTCAGACTGGTC CGAATCCAC	CCAAGATCTAAGA ACTGACGAGCG
<i>DLK1</i>	CACATGCTGCGGA AGAAGAAGAAC	ACCGCGTATACTAA GCTCTGAGGA

rRNA (18S rRNA from PE Applied Biosystems) was used as an internal control. All PCR reactions were done at least in duplicate and cycled in the GeneAmp 5700 Sequence Detection System: 50.0°C for 2 minutes, 95.0°C for 10 minutes, and 40 cycles of 95.0°C for 15 seconds and 60.0°C for 1 minute. The quantity of the specific genes obtained from standard curves was normalized to that of the 18S rRNA of the same sample. Fold change of each gene was calculated as the ratio of the mean of the normalized mRNA of nonfunctional compared with that of the normal pituitary controls.

Two-dimensional gel electrophoresis of pituitary proteins. The detailed experimental protocols have been published (18, 19). Briefly, each whole control pituitary tissue (0.45–0.70 g; $n = 8$) and each adenoma tissue (15–75 mg; $n = 11$) was homogenized and lyophilized, and the protein content was measured. For an 18-cm IPG strip, pH 3 to 10 nonlinear (Amersham Pharmacia Biotech, Piscataway, NJ), a total of 70 μg of pituitary protein was used for two-dimensional gel electrophoresis. Isoelectric focusing was done on a Multiphor II instrument (Amersham Pharmacia Biotech) with precast IPG strips (pH 3–10, nonlinear, $180 \times 3 \times 0.5$ mm). SDS-PAGE was done on a PROTEAN plus Dodeca Cell (Bio-Rad, Hercules, CA) that can analyze up to 12 gels at a time with a 12% PAGE resolving gel ($190 \times 205 \times 1.0$ mm) that was

cast with a PROTEAN plus Multicasting Chamber (Bio-Rad). The two-dimensional gel electrophoresis-separated proteins were visualized with a modified silver-staining method. The differential spots were determined between control pituitaries ($n = 8$, number of gels = 30) versus NF⁺ ($n = 2$, number of gels = 6), LH⁺ ($n = 3$, number of gels = 9), FSH⁺ ($n = 3$, number of gels = 9), FSH⁺ and LH⁺ ($n = 3$, number of gels = 9).

Image analysis of digitized two-dimensional gels. The silver-stained two-dimensional gels were digitized, and the digitized gels were analyzed qualitatively and quantitatively with the PDQuest two-dimensional Gel Analysis software for a PC computer (version 7.1.0, Bio-Rad). The total density in a gel image was used to normalize each spot volume in the gel image to minimize the effect of any experimental factor on the quantitative analysis

(19–21). Gel images in the match set were grouped into the following: control, NF⁺, LH⁺, FSH⁺, and FSH⁺ and LH⁺. The comparison analyses were done with the average normalized-volume among the five groups.

Mass spectrometry characterization of proteins. Each differential spot was labeled, excised from the two-dimensional gels, and subjected to in-gel trypsin digestion (18). That mixture of tryptic peptides was purified with a ZipTipC18 microcolumn (ZTC18S096, Millipore, Bedford, MA) according to the manufacturer's instructions. The purified tryptic-peptide mixture was analyzed with a Perseptive Biosystems matrix-assisted laser desorption/ionization time-of-flight (MALDI-TOF) Voyager DE-RP mass spectrometer (Framingham, MA) and with an LCQ^{Deca} mass spectrometer (LC-ESI-Q-IT) equipped with a standard electrospray source

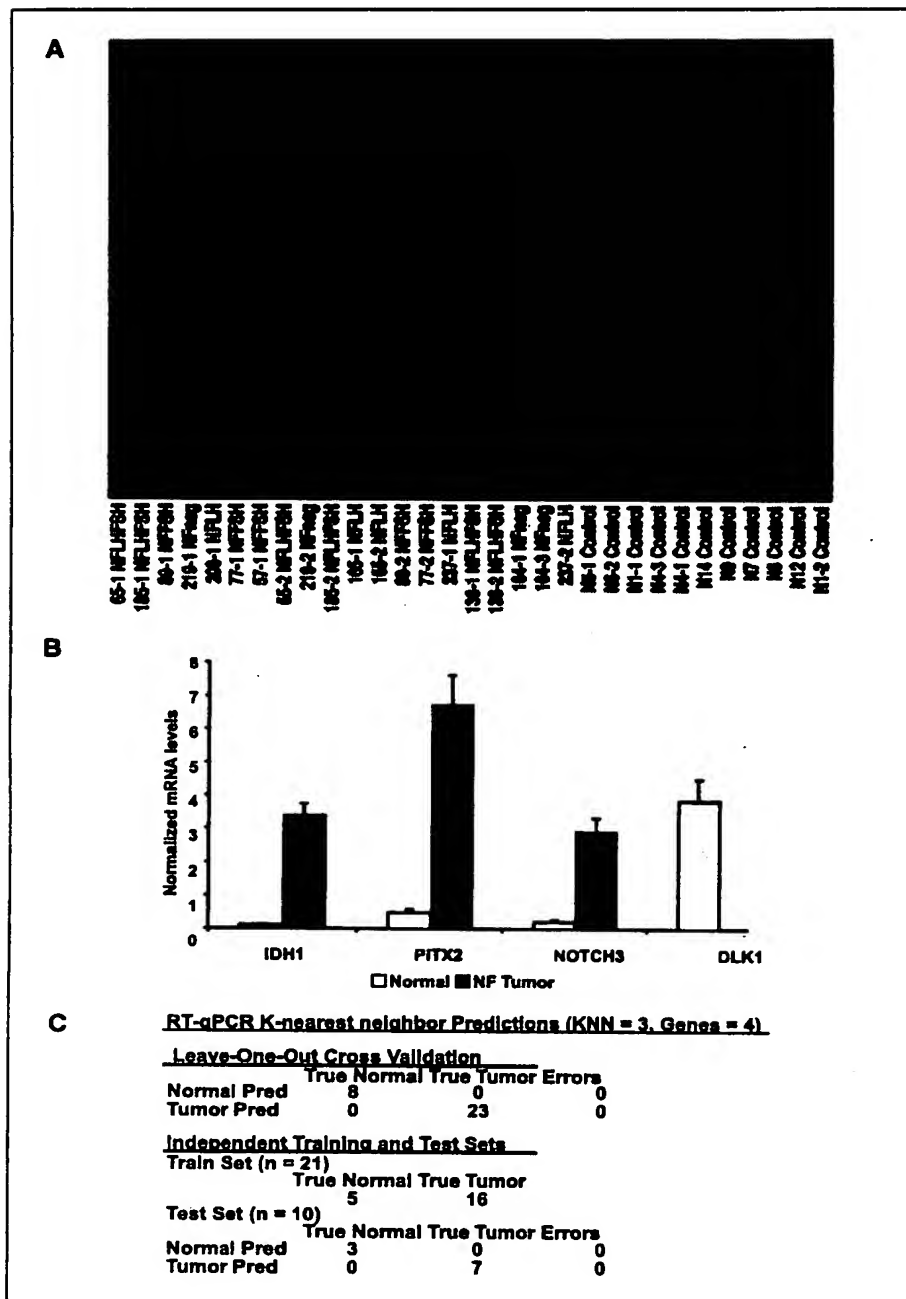


Figure 1. *A*, expression pattern of genes that are significantly different between nonfunctional pituitary adenomas and normal pituitary tissues analyzed by two-dimensional hierarchical clustering. Red, higher expression; green, lower expression; black, nonsignificant genes. *B*, RT-qPCR of relative expression of IDH1, PITX2, NOTCH3, and DLK1 mRNAs in nonfunctional adenomas ($n = 23$) compared with normal pituitaries ($n = 8$). Columns, mean mRNA expression of each gene in nonfunctional tumors or normal pituitary glands; bars, SE. Increased expression for IDH1 (41-fold), PITX2 (14-fold), and NOTCH3 (14-fold) were all confirmed by RT-qPCR. Decreased expression for DLK1 was also confirmed (~717-fold). *C*, prediction results of KNN analysis using RT-qPCR data for IDH1, PITX2, NOTCH3, and DLK1. Predictions generated with GenePattern software were 100% correct with both leave-one-out cross-validation and with independent training and test sets.

Table 2. Expression changes of selected genes in nonfunctional adenomas

Probe set ID	Symbol	Gene name	Gene Ontology category	Fold change
39930_at	<i>EPHB6</i>	EphB6	Signal transduction	15.09
203_at	<i>GATA2</i>	GATA binding protein 2	Transcription	14.55
35243_at	<i>PCTK3</i>	PCTAIRE protein kinase 3	Cell cycle	14.07
39023_at	<i>IDH1</i>	Isocitrate dehydrogenase 1 (NADP+), soluble	Metabolism	13.10
40511_at	<i>GATA3</i>	GATA binding protein 3	Transcription	12.76
41014_s_at	<i>PITX2</i>	Paired-like homeodomain transcription factor 2	Transcription	12.44
821_s_at	<i>FOLR1</i>	Folate receptor 1 (adult)	Transport	5.66
424_s_at	<i>FGFR1</i>	Fibroblast growth factor receptor 1	Signal transduction	4.27
38750_at	<i>NOTCH3</i>	Notch homologue 3	Transcription	4.26
2054_g_at	<i>CDH2</i>	N-cadherin	Cell adhesion	3.23
32565_at	<i>SMARCD3</i>	SWI/SNF related d3	Transcription	3.00
37920_at	<i>PITX1</i>	Paired-like homeodomain transcription factor 1	Transcription	2.92
469_at	<i>EFNB3</i>	Ephrin-B3	Cell-cell signaling	2.42
871_s_at	<i>HLF</i>	Hepatic leukemia factor	Transcription	2.34
41715_at	<i>PIK3C2B</i>	Phosphoinositide-3-kinase, class 2, beta	Signal transduction	2.26
823_at	<i>CX3CL1</i>	Chemokine (C-X3-C motif) ligand 1	Cell motility	2.24
40837_at	<i>TLE2</i>	Transducin-like enhancer of split 2	Development	2.03
33596_at	<i>SPOCK3</i>	Testican 3	Integral membrane	2.01
41536_at	<i>ID4</i>	Inhibitor of DNA binding 4	Transcription	-2.18
33904_at	<i>CLDN3</i>	Claudin 3	Cell adhesion	-2.47
1586_at	<i>IGFBP3</i>	Insulin-like growth factor binding protein 3	Apoptosis	-2.59
1909_at	<i>BCL2</i>	B-cell CLL/lymphoma 2	Apoptosis	-2.71
41839_at	<i>GAS1</i>	Growth arrest-specific 1	Cell cycle	-3.62
38010_at	<i>BNIP3</i>	BCL2/adenovirus E1B 19-kDa interacting protein 3	Apoptosis	-3.85
37043_at	<i>ID3</i>	Inhibitor of DNA binding 3	Transcription	-4.10
36199_at	<i>DAP</i>	Death-associated protein	Apoptosis	-4.56
40570_at	<i>FOXA1A</i>	Forkhead box O1A (rhabdomyosarcoma)	Transcription	-5.79
37005_at	<i>NBL1</i>	Neuroblastoma, suppression of tumorigenicity 1	Oncogenesis	-6.08
32786_at	<i>JUNB</i>	jun B proto-oncogene	Transcription	-6.12
39822_s_at	<i>GADD45B</i>	Growth arrest and DNA damage-inducible, β	Signal transduction	-6.24
41215_s_at	<i>ID2</i>	Inhibitor of DNA binding 2	Transcription	-6.30
39352_at	<i>CGA</i>	Glycoprotein hormones, α polypeptide	Cell-cell signaling	-7.53
31874_at	<i>GAS2L1</i>	Growth arrest-specific 2 like 1	Cell cycle	-9.04
36617_at	<i>ID1</i>	Inhibitor of DNA binding 1	Transcription	-9.73
35378_at	<i>LHB</i>	LH β polypeptide	Hormone	-12.96
1916_s_at	<i>FOS</i>	v-fos osteosarcoma viral oncogene homologue	Transcription	-15.90
649_s_at	<i>CXCR4</i>	Chemokine (C-X-C motif) receptor 4	Cell motility	-16.36
36784_at	<i>CSHL1</i>	Chorionic somatomammotropin hormone-like 1	Hormone	-85.03
878_s_at	<i>PRL</i>	Prolactin	Hormone	-100.81
40544_g_at	<i>ASCL1</i>	Achaete-scute complex-like 1 (<i>Drosophila</i>)	Neurogenesis	-116.82
40316_at	<i>GH2</i>	Growth hormone 2	Hormone	-307.69
309_f_at	<i>GH2</i>	Growth hormone 2	Hormone	-578.03
32648_at	<i>DLKI</i>	Delta-like 1 homologue (<i>Drosophila</i>)	Development	-917.43
1332_f_at	<i>GH1</i>	Growth hormone 1	Hormone	-5,000.00

(ThermoFinnigan, San Jose, CA). For MALDI-TOF MS analysis, the peptide-mass fingerprinting (PMF) data were generated. For liquid chromatography electrospray ionization ion-quadrupole-ion trap (LC-ESI-Q-IT) analysis, the amino acid sequence of each LC-separated tryptic peptide was obtained. The MALDI-TOF MS PMF data were used to identify the protein by searching the SWISS-PROT/TrEMBL database with PeptIdent software (<http://us.expasy.org/tools/peptident.html>). The LC-ESI-Q-IT tandem MS (MS/MS) data were used to identify the protein by searching the SWISS-PROT and NCBI databases with the SEQUEST software that is a part of the LCQ^{Decoa} software package.

Results

The clinical and pathologic characteristics of all nonfunctional pituitary tumors in this study are summarized in Supplementary

Table 1. The 11 pituitary tumors used in microarray analysis included tumors immunohistochemically negative for anterior pituitary hormones (NF⁻, $n = 2$), positive for luteinizing hormone (LH⁺, $n = 3$), positive for follicle-stimulating hormone (FSH⁺, $n = 3$), and positive for both FSH and LH (FSH⁺ and LH⁺, $n = 3$). These same 11 tumors were used in proteomic and RT-qPCR analyses. A total of 23 nonfunctional tumors were used for RT-PCR analysis (Supplementary Table 1).

Cluster analysis of gene expression by microarray analysis. Data from two replicate hybridizations (57-2 and 208-2) were of poor quality and removed from the analysis. To identify genes that were differentially expressed between tumor and normal pituitary samples in a statistically significant manner, we used the SAM software (17). Using a highly conservative threshold (fold change

> 2.0, FDR < 1%), we identified 297 probe sets corresponding to 284 unique genes that were significantly different between pituitary tumors and normal tissues. Normalized expression data from these 297 probe sets were analyzed by two-dimensional hierarchical clustering (Fig. 1A). A complete list of these 284 unique genes is given in Supplementary Table 2, and a subset of those genes is provided in Table 2. In general, tumor suppressors (e.g., *NBL1*) and apoptosis inducers (*BNIP3*) were down-regulated, whereas antiapoptotic genes (*PIK3C2B* and *FAIM2*) were up-regulated. In addition, the apoptosis inhibitor *BCL2* was down-regulated by >3-fold compared with normal pituitary, suggesting that other antiapoptotic mechanisms are at work in nonfunctional pituitary adenomas. Positive regulators of cell cycle progression, such as PCTAIRE protein kinase 3, exhibited an increased expression, whereas negative cell cycle regulators, such as *GADD45B* and *GAS1*, were down-regulated.

Two components of the delta-Notch pathway, NOTCH3 and DLK1, were strongly altered in opposite directions. NOTCH3 was up-regulated nearly 5-fold, whereas DLK1 was repressed over 900-fold. In addition, human achaete-scute homologue (ASCL1/HASH1), which is essential for DLK1 expression, was down-regulated over 100-fold. The fibroblast growth factor receptor 1 (FGFR1) was up-regulated over 3-fold in nonfunctional pituitary adenomas. In addition, expression of the insulin-like growth factor binding protein 3 (IGFBP3), which decreases IGF availability and signaling, was reduced 3-fold compared with normal tissues.

Over 50 transcription factors were altered in their expression in nonfunctional pituitary adenomas, making it one of the largest functional categories (Supplementary Table 2). Several developmental transcription factors, including NOTCH3, PITX1, PITX2, and PBX3, were up-regulated, whereas others, such as C/EBP δ were

down-regulated. Surprisingly, the inhibitors of the DNA-binding family (ID1, ID2, ID3, and ID4), which are inhibitors of neural differentiation and are frequently overexpressed in neuroectodermal tumors (22), were all down-regulated in pituitary adenomas. Some transcription factors associated with oncogenesis, such as FOS, JUNB, and FOXO1A/FKHR, were also down-regulated. Nevertheless, decreased levels of FOXO1A/FKHR are consistent with an elevated signaling through the phosphatidylinositol 3-kinase/PTEN/AKT pathway, because AKT activation results in the exclusion of FKHR from the nucleus (23).

Several genes that enhance cell motility and invasion were increased in nonfunctional pituitary adenomas, including *ephrin receptor B6*, *ephrin B3*, *testican 3*, *N-cadherin 2*, and the chemokine ligand *CX3CL1*. The down-regulation of the tight-junction molecule claudin 3 was consistent with a cellular phenotype of increased motility. Moreover, our gene expression profiling results were consistent with the expectations for the nonfunctional tumors. For example, the up-regulation of the folate receptor (FOLR1) was consistent with our previous observations (15, 16). In addition, LH, growth hormone 1, growth hormone 2, chorionic somatomammotropin hormone-like 1, and prolactin were all strongly down-regulated as expected.

Validation of expression array result by reverse transcription real-time quantitative PCR analysis. To validate the microarray analysis, we measured with RT-qPCR, using SYBR Green I dye detection the mRNA expression levels of IDH1, PITX2, NOTCH3, and DLK1 using blinded samples which consisted of 23 non-functional tumors and eight normal pituitary glands. The 23 nonfunctional tumors composed of six FSH $^+$, six LH $^+$, six FSH $^+$ and LH $^+$, and five NF $^-$ (Supplementary Table 1). Using blinded samples

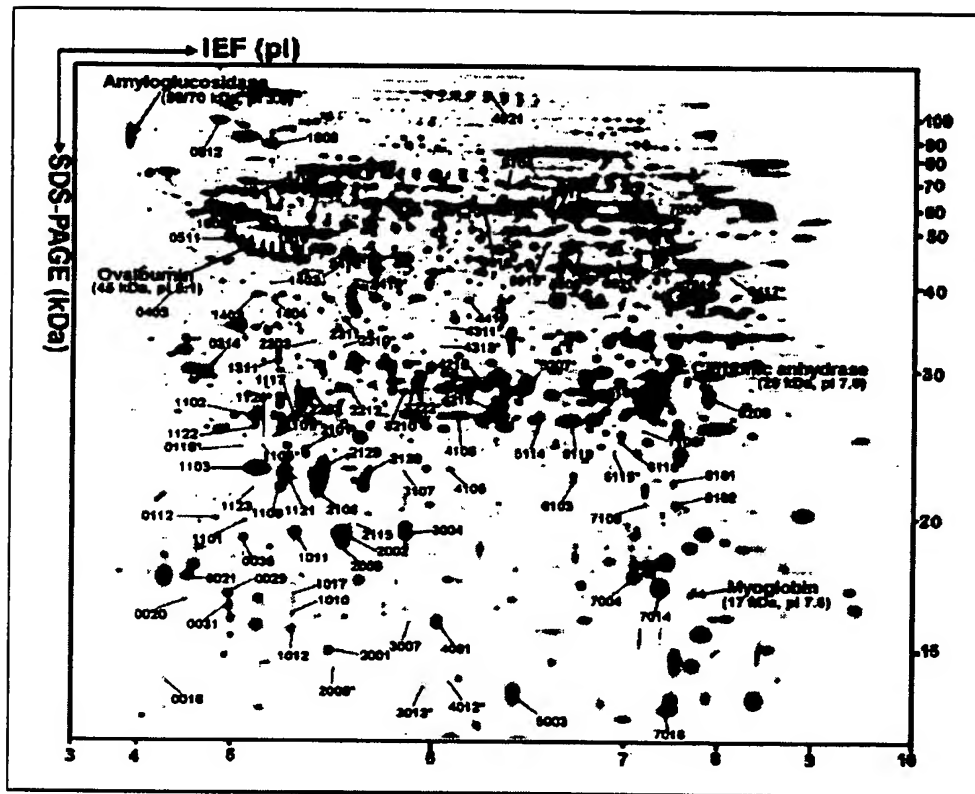


Figure 2. A digitized two-dimensional gel electrophoresis reference map (Gaussian image) from a human control pituitary proteome labeled with the 93 differential spots and the four protein standard markers. Isoelectric focusing (IEF) was done with an 18-cm IPG strip (pH 3-10, nonlinear), and vertical SDS-PAGE was done with a 12% polyacrylamide gel.

Table 3. Molecular classification of nonfunctional tumors by subtype by gene expression profile analysis

Subtype	Fold change	Gene symbol	Probe set ID	Accession no.	Title
FSH ⁺	4.7	<i>CXCL13</i>	41104_at	NM_006419	Chemokine (C-X-C motif) ligand 13
FSH ⁺	2.7	<i>HPIP</i>	38063_at	NM_020524	Hematopoietic PBX-interacting protein
FSH ⁺	2.2	<i>KRT19</i>	40899_at	NM_002276	Keratin 19
LH ⁺	4.5	<i>MLP</i>	36174_at	NM_023009	MARCKS-like protein
LH ⁺	2.7	<i>GUCY1A3</i>	36918_at	NM_000856	Guanylate cyclase 1, soluble, α 3
LH ⁺	2.4	<i>TMPRSS6</i>	34067_at	NM_153019	Type II transmembrane serine protease 6
LH ⁺	2.4	<i>BASPI</i>	32607_at	NM_006317	Brain abundant, membrane attached signal protein 1
NF ⁻	15.9	<i>C7</i>	37394_at	NM_000587	Complement component 7
NF ⁻	5.9	<i>PDLIM1</i>	36937_s_at	NM_020992	PDZ and LIM domain 1 (elfin)
NF ⁻	4.6	<i>HIST1H2AC</i>	34308_at	NM_003512	Histone 1, H2ac
NF ⁻	4.1	<i>GPR49</i>	41073_at	NM_003667	G protein-coupled receptor 49
NF ⁻	3.9	<i>SYT1</i>	40075_at	NM_005639	Synaptotagmin I
NF ⁻	3.7	<i>ALS2CR3</i>	40064_at	NM_015049	Amyotrophic lateral sclerosis 2, candidate 3
NF ⁻	3.6	<i>HIST1H2BL</i>	35576_f_at	NM_003519	Histone 1, H2bl
NF ⁻	3.3	<i>HIST2H2AA</i>	286_at	NM_003516	Histone 2, H2aa
NF ⁻	3.1	<i>HIST1H2BN</i>	36347_f_at	NM_003520	Histone 1, H2bn
NF ⁻	3.0	<i>PTPN3</i>	31885_at	NM_002829	Protein tyrosine phosphatase, nonreceptor type 3
NF ⁻	2.3	—	34114_at	AL109678	cDNA clone EUROIMAGE 28993.
NF ⁻	2.2	<i>HIST1H2BM</i>	31528_f_at	NM_003521	Histone 1, H2bm
NF ⁻	2.2	<i>HIST1H2BK</i>	32819_at	NM_080593	Histone 1, H2bk
NF ⁻	2.2	<i>AGPAT1</i>	32836_at	NM_006411	1-Acylglycerol-3-phosphate <i>O</i> -acyltransferase 1

NOTE: Genes that were altered specifically in each subtype of nonfunctional adenomas are shown. NF⁻, negative immunohistochemical stains for ACTH, LH, FSH, PRL, GH, and TSH.

Adenomas were graded blindly by a neuropathologist from 0 to 4 for intensity of staining for each peptide hormone.

to do RT-qPCR, the normalized value of each gene of each sample was used to classify the sample in two groups (nonfunctional and control groups) correctly. RT-qPCR analysis showed that IDH1, PITX2, and NOTCH3 mRNAs were significantly up-regulated respectively 41-fold, 14-fold, and 14-fold in nonfunctional pituitary adenomas, and that DLK1 mRNA expression was down-regulated 717-fold (Fig. 1C).

We next used the RT-qPCR data to attempt to classify the nonfunctional tumor and normal samples using the KNN method. With the GenePattern software (<http://www.broad.mit.edu/cancer/software/genepattern/>), the tumor and normal samples were correctly predicted in 100% of the cases using the normalized RT-qPCR data for these four genes (Fig. 1C). This level of accuracy was achieved both with leave-one-out cross-validation and when the data was separated into independent training sets ($n = 21$) and test sets ($n = 10$).

Proteomic analysis of human nonfunctional pituitary adenoma and control samples. The proteomes from control pituitary versus NF⁻, LH⁺, FSH⁺, and FSH⁺ and LH⁺ tumors were analyzed by two-dimensional gel electrophoresis. Each sample was analyzed three to five times, and ca. 1,000 protein spots were detected in each gel (Fig. 2 contains a digital master gel map). For each sample, the correlation coefficient (r) of the normalized volumes between-gel matched spots was >0.73 (range, 0.76–0.92), and the mean between-gel, matched percentage was 85% to 99% for the controls and 81% to 90% for the adenomas. A total of 93 differential protein spots were found among the different cell types of nonfunctional adenomas. Each differential spot was labeled in the digital master gel map (Fig. 2). Supplementary Table 3 contains those MS-characterized protein spots for which the spot volume in

the control group was significantly different from each adenoma group ($P < 0.001$). Differential spots were excised, in-gel trypsin digestion was done, and MS (MALDI-TOF PMF and/or LC-ESI-Q-IT MS/MS) was used to characterize the protein in each differential spot (18). Among those 93 differential spots, 72 spots contained 50 differentially regulated proteins (21 up-regulated and 29 down-regulated) that were characterized. MS/MS data were used to search the database with SEQUEST software.

The 50 MS-characterized differentially expressed proteins were categorized into several different functional groups (Supplementary Table 3). Identified proteins that were affected in nonfunctional adenomas included the following: (a) Neuroendocrine-related proteins, including somatotropin, secretogogin, and mu-crystallin homologue, were down-regulated in the nonfunctional pituitary adenomas. (b) At least 17 isoforms of somatotropin were down-regulated. (c) Immunologic regulation proteins and tumor-related antigen (immunoglobulin, tumor rejection antigen 1) were down-regulated. (d) Cell proliferation, differentiation, and apoptosis-related proteins were down-regulated. (e) Cell defense and stress resistance proteins (phospholipid hydroperoxide glutathione peroxidase, CD59 glycoprotein, and heat shock 27-kDa protein) were down-regulated. (f) Some metabolic enzyme-related proteins (IDH [NADP] cytoplasmic, tryptophan 5-hydroxylase 2, matrix metalloproteinase-9, aldose reductase, lactoylglutathione lyase, acyl-CoA-binding protein) were up-regulated in the nonfunctional pituitary adenomas.

Proteomic validation of gene expression profiling data. We compared the proteomic data with gene expression profiling data for consistency at the protein and the mRNA levels. Whereas expression profiling identified 284 altered genes, proteomics

identified 50 altered proteins (10.7%). Of these 50 proteins, only 40 had corresponding probe sets present on the U95A GeneChip. Of those 40 detectable genes, 31 genes (77.5%) were detected as present at the mRNA level. Four of these genes (*IDH1*, *GH1*, *GH2*, and *PRL*) met our mRNA significance criteria and were identified by both experimental approaches. Thirteen additional genes (32.5%) did not meet our significance criteria but nevertheless had mRNA changes of >1.3-fold in the same direction as observed changes at the protein level. Only one gene (*Thioredoxin domain containing 9*, O14530) had opposite changes and was decreased at the protein level but increased (1.32-fold) at the mRNA level. Finally, 32.5% of the altered proteins showed essentially no change at the mRNA level. In general, there was quite good agreement between the proteomics and expression data (43%), although not surprisingly, there were proteins with altered abundance that showed little if any change at the level of transcription. These genes are likely regulated by altered translational efficiencies and posttranslational effects on protein stabilities.

Molecular classification of nonfunctional pituitary tumors by subtype. We further analyzed the gene expression profiles of all four nonfunctional pituitary subtypes to each other and identified genes that were affected uniquely in each subtype (Table 3). To qualify for this description, the genes had to be significantly different in only a single subtype relative to normal tissue and also be significantly different between that tumor subtype and the other tumor subtypes. No genes were uniquely altered in the nonfunctional tumors that expressed both the LH⁺ and FSH⁺ subtype. In the nonfunctional tumors that expressed FSH⁺ subtype, *CXCL13* and hematopoietic PBX-interacting protein were up-regulated. In the nonfunctional tumors that expressed LH⁺ subtype, uniquely up-regulated genes included *MLP*, *GUCY1A3*, *TMPRSS6*, and *BASPI*. In the NF⁻ subtype tumors, 14 genes were uniquely up-regulated, including four Histone 2b variants, two Histone 2a variants, and *synaptotagmin I*.

Discussion

Our gene expression profiling of nonfunctional pituitary adenomas identified 115 up-regulated genes and 169 down-regulated genes. Some gene profiles showed good agreement with the proteomic data. In addition, the gene expression data were consistent with expected results for a number of genes, such as *FOLR1*, *growth hormone*, and prolactin *Pit-1*. The RT-qPCR results of all four genes tested (*IDH1*, *PITX2*, *NOTCH3*, and *DLK1*) confirmed our gene expression profiling data.

We observed increased levels of *IDH1* mRNA by gene expression profiling, RT-qPCR, and proteomic analysis. IDHs (24) catalyze oxidative decarboxylation of isocitrate into α-ketoglutarate. In addition, mitochondrial and cytosolic NADP(+)-dependent IDHs play an important role in cellular defense against oxidative damage as a source of NADPH (25, 26). Moreover, NADP-dependent IDH is up-regulated in human colon tumors (27) and may prevent apoptosis in tumors cells via detoxification of tumor therapeutic drugs (28).

Our observation that *PITX2* is overexpressed in nonfunctional pituitary adenomas is consistent with previous analyses of human pituitary adenomas (29). *PITX1* (also known as *P-OTX*) and *PITX2* specify closely related bicoid transcription factors that appear early, are made in multiple tissues, and continue to be expressed in adult life (30, 31). *PITX2a* and *PITX1* both interact with *Pit-1*, a master regulator of pituitary cell differentiation, thyroid-stimulating hormone, growth hormone, and prolactin genes (31, 32).

Normally, *PITX2* mRNA displays a rapid turnover rate, but activation of the Wnt/β-catenin pathway stabilizes *PITX2* mRNA (33). In fact, *PITX2* is rapidly induced by the Wnt/Dvl/β-catenin pathway and is required for effective cell type-specific proliferation during pituitary development by directly activating cyclin D2 expression (34). Regulated exchange of HDAC1/β-catenin converts *PITX2* from repressor to activator, analogous to the control of TCF/LEF1. *PITX2* serves as a competence factor that is required for the temporally ordered and growth factor-dependent recruitment of a series of specific coactivator complexes that prove necessary for cyclin D2 and cyclin D1 (35) gene induction. Although we observed increased cyclin D1 levels, cyclin D2 expression was not increased. In addition, *SFRP1* levels were up-regulated 9-fold, and *SFRP1* has been shown to be capable of increasing Wnt signaling rather than antagonizing it in some conditions (36, 37). Taken together, the changes we observed in *SFRP1*, *PITX2*, and cyclin D1 are all consistent with a model in which elevated Wnt/β-catenin signaling is important for nonfunctional pituitary adenomas (Fig. 3). Moreover, increased nuclear accumulation of β-catenin has been detected by immunohistochemistry in 57% of pituitary adenomas (38), consistent with our conclusion that the Wnt/β-catenin pathway is important in the progression of this malignancy.

NOTCH3 is strongly overexpressed, whereas *DLK1*, a potential ligand of *NOTCH3*, was one of the most strongly down-regulated gene in nonfunctional tumors. Members of the delta family serve as ligands in cell-to-cell interactions with Notch receptors that control cell fate during differentiation. Interaction of Notch receptors with their cell-bound ligands results in the proteolytic cleavage of Notch, translocation of the intracellular domain (Notch-IC) to the nucleus, and altered gene expression. Emerging data also support the role of the Notch signaling pathway in tumorigenesis and neural development. Constitutive expression of *NOTCH3-IC* in the peripheral epithelium in the developing lung of transgenic mice resulted in altered lung morphology and delayed development, suggesting that *NOTCH3* signaling could contribute to lung cancer

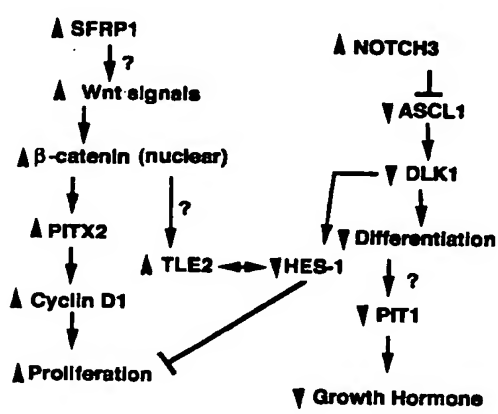


Figure 3. A model of the effects of Wnt and Notch signaling on nonfunctional pituitary adenomas. Genes with an increased mRNA level (*up arrow*) and with a decreased expression (*down arrow*). In this model, increased *SFRP1* activates the Wnt pathway, resulting in nuclear β-catenin, increased *PITX2*, elevated cyclin D1, and cellular proliferation. In parallel, increased *NOTCH3* represses *HES1/ASCL1*, resulting in reduced *DLK1* and inhibiting cellular differentiation, and *PIT1* and *GH* expression. How increased *TLE2* and decreased *HES-1* levels affect tumor progression requires further investigation but may enhance proliferation and inhibit differentiation.

progression through the inhibition of terminal differentiation (39). Moreover, transgenic mice expressing NOTCH3-IC in thymocytes and T cells developed early and aggressive T-cell neoplasias (40). NOTCH3 and DLK1 expression is inversely correlated in neuroblastoma cell lines that can be divided into two groups with high DLK1/low NOTCH3 expression, or high NOTCH3/low DLK1 expression (41). Importantly, this study found a perfect correlation of mRNA and protein levels for both NOTCH3 and DLK1 (41). In neuroendocrine cell differentiation, changes in DLK1 levels seem to mark the decision to mature along different lineages. Thus, the high levels of NOTCH3 and low levels of DLK1 in nonfunctional pituitary adenomas suggest that they are derived from earlier-stage, undifferentiated cells, or that they have taken on a dedifferentiated state, consistent with the loss of Pit-1 expression.

The nonfunctional adenoma cells seem to have switched from a delta-expressing cell type to a Notch-expressing cell type and might receive stimulatory signals from neighboring normal pituitary cells that still express DLK1. This hypothesis suggests that inhibitors of Notch processing, such as γ -secretase inhibitors that were developed for Alzheimer's therapies and are now in clinical trials to treat Notch-activated T-cell acute lymphoblastic leukemia (42), could also prove of benefit to patients with nonfunctional pituitary adenomas.

Another gene involved in the delta-Notch pathway that was strongly down-regulated in nonfunctional adenomas was ASCL1. In *Drosophila*, Achaete-Scute genes are upstream of and directly

activate the expression of delta and Notch (43), and in developing mouse neuroendocrine cells, DLK1 expression depends on the mouse Achaete-Scute homologue (44). Furthermore, high levels of Notch signaling can induce the transcriptional silencing of ASCL1 (45). Thus, the high levels of NOTCH3 could repress ASCL1 leading to the loss of DLK1 expression in nonfunctional adenomas. Transducin-like enhancer of split 2 (TLE2) is a mammalian homologue of the *Drosophila* transcriptional repressor *groucho*, which represses targets of β -catenin. TLE2 interacts with HES-1 and is expressed during neuronal development (46). Thus, TLE2, which was up-regulated 2-fold in nonfunctional adenomas, is a link between Wnt-signaling and Notch signaling. These data support a model (Fig. 3) in which NOTCH3 represses HASH1 and in cooperation with Wnt signaling, NOTCH3 maintains in these tumors in an undifferentiated state.

Acknowledgments

Received 3/16/2005; revised 8/3/2005; accepted 9/3/2005.

Grant support: Department of Neurosurgery (N.M. Oyesiku), NIH grants K22-CA96560 (C.S. Moreno) and R01-CA106826 (C.S. Moreno), NS 42843 (D.M. Desiderio), RR-10522 (D.M. Desiderio), RR-14593 (D.M. Desiderio), and NSF DBI 9604633 (D.M. Desiderio).

The costs of publication of this article were defrayed in part by the payment of page charges. This article must therefore be hereby marked *advertisement* in accordance with 18 U.S.C. Section 1734 solely to indicate this fact.

We thank the Department of Neuropathology, Emory University Hospital for the histology and immunohistochemistry analyses.

References

- Greenman Y, Melmed S. Diagnosis and management of nonfunctioning pituitary tumors. *Annu Rev Med* 1996;47:95–106.
- Ara SL, Ezzat S. The cytogenesis and pathogenesis of pituitary adenomas. *Endocr Rev* 1998;19:798–827.
- Ara SL, Kovacs K. Clinically non-functioning human pituitary adenomas. *Can J Neurol Sci* 1992;19:228–35.
- Black PM, Iusu DW, Klibanski A, et al. Hormone production in clinically nonfunctioning pituitary adenomas. *J Neurosurg* 1987;66:244–50.
- Katznelson L, Alexander JM, Klibanski A. Clinical review 45: clinically nonfunctioning pituitary adenomas. *J Clin Endocrinol Metab* 1993;76:1089–94.
- Herman V, Fagin J, Gonsky R, Kovacs K, Melmed S. Clonal origin of pituitary adenomas. *J Clin Endocrinol Metab* 1990;71:1427–33.
- Alexander JM, Biller BM, Bikkal H, Zervas NT, Arnold A, Klibanski A. Clinically nonfunctioning pituitary tumors are monoclonal in origin. *J Clin Invest* 1990;86:336–40.
- Evans CO, Brown MR, Parks JS, Oyesiku NM. Screening for MEN1 tumor suppressor gene mutations in sporadic pituitary tumors. *J Endocrinol Invest* 2000;23:304–9.
- Satta MA, Korbonits M, Jacobs RA, et al. Expression of menin gene mRNA in pituitary tumors. *Eur J Endocrinol* 1999;140:358–61.
- Farrell WE, Simpson DJ, Bicknell J, et al. Sequence analysis and transcript expression of the MEN1 gene in sporadic pituitary tumours. *Br J Cancer* 1999;80:44–50.
- Shimon L, Melmed S. Genetic basis of endocrine disease: pituitary tumor pathogenesis. *J Clin Endocrinol Metab* 1997;82:1675–81.
- Spada A, Faglia G. G-protein dysfunction in pituitary tumors. In: Melmed S., editor. *Oncogenesis and molecular biology of pituitary tumors*. Vol. 20. Basel: Karger; 1996. p. 108–21.
- Gittles NJ. Current perspectives on the pathogenesis of clinically non-functioning pituitary tumors. *J Endocrinol* 1998;157:177–86.
- Chaidarun SS, Eggo MC, Sheppard MC, Stewart PM. Expression of epidermal growth factor (EGF), its receptor, and related oncoprotein (erbB-2) in human pituitary tumors and response to EGF *in vitro*. *Endocrinology* 1994;135:2012–21.
- Evans CO, Reddy P, Brat DJ, et al. Differential expression of folate receptor in pituitary adenomas. *Cancer Res* 2003;63:4218–24.
- Evans CO, Young AN, Brown MR, et al. Novel patterns of gene expression in pituitary adenomas identified by complementary deoxyribonucleic acid microarray and quantitative reverse transcription-polymerase chain reaction. *J Clin Endocrinol Metab* 2001;86:3097–107.
- Tusher VG, Tibshirani R, Chu G. Significance analysis of microarrays applied to the ionizing radiation response. *Proc Natl Acad Sci U S A* 2001;98:5116–21.
- Zhan X, Desiderio DM. A reference map of a human pituitary adenoma proteome. *Proteomics* 2003;3:699–713.
- Zhan X, Desiderio DM. Spot volume vs. amount of protein loaded onto a gel: a detailed, statistical comparison of two gel electrophoresis systems. *Electrophoresis* 2003;24:1818–33.
- Zhan X, Desiderio DM. Differences in the spatial and quantitative reproducibility between two second-dimensional gel electrophoresis systems. *Electrophoresis* 2003;24:1834–46.
- Zhan X, Desiderio DM. Heterogeneity analysis of the human pituitary proteome. *Clin Chem* 2003;49:1740–51.
- Iavarone A, Lasorella A. Id proteins in neural cancer. *Cancer Lett* 2004;204:189–96.
- Nakamura N, Ramaswamy S, Vazquez F, Signoretto S, Loda M, Sellers WR. Forkhead transcription factors are critical effectors of cell death and cell cycle arrest downstream of PTEN. *Mol Cell Biol* 2000;20:8969–82.
- Haselbeck RJ, McAlister-Henn L. Function and expression of yeast mitochondrial NAD- and NADP-specific isocitrate dehydrogenases. *J Biol Chem* 1993;268:12116–22.
- Jo SH, Son MK, Koh HJ, et al. Control of mitochondrial redox balance and cellular defense against oxidative damage by mitochondrial NADP-dependent isocitrate dehydrogenase. *J Biol Chem* 2001;276:16168–76.
- Kim SY, Park JW. Cellular defense against singlet oxygen-induced oxidative damage by cytosolic NADP-dependent isocitrate dehydrogenase. *Free Radic Res* 2003;37:309–16.
- Mazurek S, Grimm H, Oehmke M, Weisse G, Teigelkamp S, Eigenbrodt E. Tumor M2-PK and glutaminolytic enzymes in the metabolic shift of tumor cells. *Anticancer Res* 2000;20:5151–4.
- Mazurek S, Weisse G, Wust G, Schafer-Schwebel A, Eigenbrodt E, Friis RR. Energy metabolism in the involuting mammary gland. *In Vivo* 1999;13:467–77.
- Pellegrini-Bouiller I, Manrique C, Gunz G, et al. Expression of the members of the Ptx family of transcription factors in human pituitary adenomas. *J Clin Endocrinol Metab* 1999;84:2212–20.
- Parks JS, Brown MR. Transcription factors regulating pituitary development. *Growth Horm IGF Res* 1999;9 Suppl B:2–8; discussion 8–11.
- Szeto DP, Ryan AK, O'Connell SM, Rosenfeld MG. P-OTX a PIT-1 interacting homeodomain factor expressed during anterior pituitary gland development. *Proc Natl Acad Sci U S A* 1996;93:7706–10.
- Simmons DM, Voss JW, Ingraham HA, et al. Pituitary cell phenotypes involve cell-specific Pit-1 mRNA translation and synergistic interactions with other classes of transcription factors. *Genes Dev* 1990;4:695–711.
- Briata P, Ilengo C, Corte G, et al. The Wnt/ β -catenin- \rightarrow Pitx2 pathway controls the turnover of Pitx2 and other unstable mRNAs. *Mol Cell* 2003;12:1201–11.
- Kioussi C, Briata P, Baek SH, et al. Identification of a Wnt/Dvl/ β -catenin- \rightarrow Pitx2 pathway mediating cell-type-specific proliferation during development. *Cell* 2002;111:673–85.
- Baek SH, Kioussi C, Briata P, et al. Regulated subset of G_i growth-control genes in response to derepression by the Wnt pathway. *Proc Natl Acad Sci U S A* 2003;100:3245–50.
- Kawano Y, Kypta R. Secreted antagonists of the Wnt signalling pathway. *J Cell Sci* 2003;116:2627–34.
- Uren A, Reichsman F, Anest V, et al. Secreted frizzled-related protein-1 binds directly to Wingless and is a biphasic modulator of Wnt signaling. *J Biol Chem* 2000;275:4374–82.
- Semba S, Han SY, Ikeda H, Horii A. Frequent nuclear accumulation of β -catenin in pituitary adenoma. *Cancer* 2001;91:42–8.

39. Dang TP, Eichenberger S, Gonzalez A, Olson S, Carbone DP. Constitutive activation of Notch3 inhibits terminal epithelial differentiation in lungs of transgenic mice. *Oncogene* 2003;22:1988-97.
40. Bellavia D, Campese AF, Checquolo S, et al. Combined expression of pTα and Notch3 in T cell leukemia identifies the requirement of preTCR for leukemogenesis. *Proc Natl Acad Sci U S A* 2002;99:3788-93.
41. Van Limpt VA, Chan AJ, Van Shuis PG, Caron HIN, Van Noesel CJ, Versteeg R. High delta-like 1 expression in a subset of neuroblastoma cell lines corresponds to a differentiated chromaffin cell type. *Int J Cancer* 2003;105:61-9.
42. Weng AP, Ferrando AA, Lee W, et al. Activating mutations of NOTCH1 in human T cell acute lymphoblastic leukemia. *Science* 2004;306:269-71.
43. Heitzler P, Bourouis M, Ruel L, Carteret C, Simpson P. Genes of the Enhancer of split and achaete-scute complexes are required for a regulatory loop between Notch and Delta during lateral signaling in *Drosophila*. *Development* 1996;122:161-71.
44. Ito T, Udaka N, Yazawa T, et al. Basic helix-loop-helix transcription factors regulate the neuroendocrine differentiation of fetal mouse pulmonary epithelium. *Development* 2000;127:3913-21.
45. Ball DW. Achaete-scute homolog-1 and Notch in lung neuroendocrine development and cancer. *Cancer Lett* 2004;204:159-69.
46. Grbavec D, Lo R, Liu Y, Stifani S. Transducin-like Enhancer of split 2, a mammalian homologue of *Drosophila* Groucho, act as a transcriptional repressor, interacts with Hairy/Enhancer of split proteins, and is expressed during neuronal development. *Eur J Biochem* 1998;258:339-49.